Tufa-Based Reconstructions of Huasco Basin Lake Levels

by

Ruth Rosegrant Tweedy

Submitted to the Department of Earth, Atmospheric and Planetary Sciences
in partial fulfillment of the requirements for the degree of

Bachelor of Science in Earth, Atmospheric and Planetary Sciences

at the

MASSACHUSETTS INSTITUTE OF TECHNOLOGY

May 20, 2020

Author .....
Department of Earth, Atmospheric and Planetary Sciences
May 20, 2020

Certified by .....
David McGee
Associate Professor
Thesis Supervisor

Accepted by .....
Richard P. Binzel
Chair, Committee on Undergraduate Program

Tufa-Based Reconstructions of Huasco Basin Lake Levels

by

Ruth Rosegrant Tweedy

Submitted to the Department of Earth, Atmospheric and Planetary Sciences
on May 20, 2020, in partial fulfillment of the
requirements for the degree of
Bachelor of Science in Earth, Atmospheric and Planetary Sciences

Abstract

This thesis investigates the Salar del Huasco (northern Chile) as a potential site for palaeohydrological reconstructions of precipitation over the South American Altiplano, and presents a preliminary lake level chronology for the last deglaciation. Resolving the timings of past lake level highstands in the South American Altiplano will ultimately provide better understanding of what climate events force the South American Summer Monsoon (SASM) further south. Better insight into the forcing mechanisms of the SASM will improve our understanding of monsoon systems, and can be applied to refine global climate models of the region. To create this lake level chronology, tufa samples deposited at different elevations within the Salar del Huasco were dated using U/Th disequilibrium dating, and stable isotope measurements were applied to examine the past hydrology of the basin. The Salar del Huasco was found to have remained a hydrologically closed basin during highstand events, meaning lake level variations within the basin are purely driven by local precipitation-evaporation balances. Furthermore, the preliminary lake level chronology broadly agrees with the timings suggested by other palaeohydrological studies from the region, and provides support for a currently controversial lake level highstand between 120-100 ka. These results imply that the Salar del Huasco accurately reflects SASM-forced lake level histories, and should be studied further.

Thesis Supervisor: David McGee
Title: Associate Professor

Acknowledgments

Firstly, I want to thank Professor David McGee for agreeing to take me on as an Undergraduate Thesis advisee, and for his dedicated support throughout the entirety of my thesis. A further thank you to all of the members of the McGee group for making me feel so welcome, but particularly to Dr. Christopher Kinsley and Dr. Adam B. Jost. They were instrumental in my getting the practical portion of my thesis done. From my initial U/Th chemistry training, to many long hours supervising me on the Mass Spec, to reducing data sheets, this thesis work would not have been finished without you!

A further thanks to Dr. Christine Y. Chen, who deserves a paragraph all to herself! Christine's endless knowledge and enthusiasm for all things tufa were the driving force behind this project. Her positivity, her faith in me, and her absolute dedication to making my science the best that it could be consistently pushed me to do better, and made this thesis what it is. Without Christine, none of this work would have been possible (she can't even argue, as she collected the samples!).

Finally, I'd like to thank my family for their constant support throughout my past four years at MIT, and during this final thesis write-up. They kept me fed, watered, and (relatively) sane as I completed this thesis. For that, and for so many other things, I'm grateful!

Contents

Chapter 1

Introduction

1.1 The South American Summer Monsoon - The Big Picture

In the South American Altiplano, approximately 50% of the economically active population practice traditional smallholder (family run, less than 1.3 ha of cropland per person) rainfed agriculture (Garcia et al., 2007; Sietz et al., 2012). Because of the high dependence of the population on water availability, it is vital to understand how rainfall patterns may differ in the future due to anthropogenic climate change. Currently, over 70% of the region's annual rainfall occurs in the austral summer (December-February), and is associated with the South American Summer Monsoon (SASM) (Garreaud et al., 2003; Minvielle and Garreaud, 2011). Therefore, in order to understand how Altiplano rainfall is likely to change in future, resolving the key parameters that affect SASM characteristics over the region is crucial.

Though there have been recent improvements in scientific understanding of forcing mechanisms that alter the strength and location of monsoons (Kanner et al., 2012; Mohtadi et al., 2016), current efforts have not been able to determine to what extent, or even in what direction (positive or negative), precipitation over the Altiplano is expected to change (Thibeault et al., 2010). Unfortunately, current global climate models are too poorly resolved to accurately model precipitation predictions for the

Altiplano. These models use grid spacings that are too large to reflect the spatial distribution of precipitation in the relatively narrow Altiplano plateau. Furthermore, there is a severe lack of palaeohydrological data for this area, meaning that regional models do not have strong records for how past forcings affected the SASM, and therefore Altiplano rainfall. This means there is huge uncertainty in how much water availability in the area will change in the future, as we do not understand what parameters primarily force the SASM (Minvielle and Garreaud, 2011; Thibeault et al., 2010).

Further understanding of the palaeohydrology of the Altiplano is essential to serve as a base for accurate modelling. One way to track past water availability is to trace lake level changes in hydrologically closed basins. Simply put, periods of higher lake levels indicate times of increased water availability. By creating a chronology of past lake levels and comparing this to different climatic forcing events, key drivers of precipitation amount can be identified. Though none of the proposed past forcers of SASM variability are direct analogues for anthropogenic climate change, these past lake level changes effectively represent natural experiments that can be used to test current understanding of the global climate events altering rainfall patterns, and so inform climate models in the future.

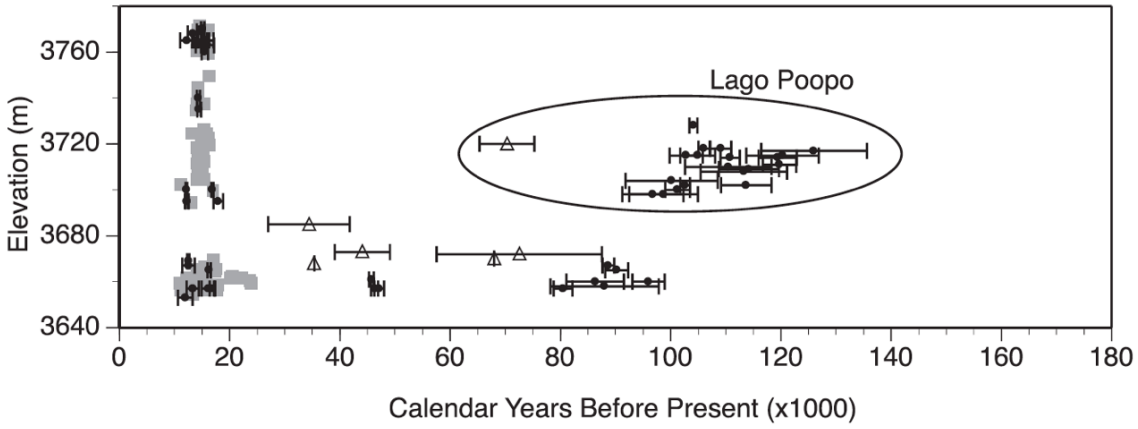

Figure 1-1: Paleolake levels for the Titicaca-Uyuni basin plotted against time (ka). Sparse records with poorly resolved dating are seen before the last glacial maximum. Black circles and grey squares correspond to U/Th and radiocarbon data (respectively) from Placzek et al. (2006), triangles correspond to 1990 thesis data. Figure from Baker and Fritz (2015).

The South American Altiplano Plateau consists of several closed drainage basins totaling a 200,000 km^2 area around 3800 m above sea level (Placzek et al., 2006; Sánchez-Saldías and Fariña, 2014). Lake carbonate deposits in the Titicaca-Uyuni system, the largest watershed in the Altiplano, indicate far higher lake levels than at present (see Figure 1-1), with the lake highstand between 18.1-14.1 ka having a surface area six times larger than modern Titicaca (Placzek et al., 2013). Currently, of the four main lake basins, the Uyuni and Coipasa basins exist only as salt flats that formed after the evaporation of the lake basins, and the Titicaca and Poopo lakes are significantly reduced in scale (Placzek et al., 2006). There is still substantial uncertainty as to what drove these past lake level fluctuations.

The key climatic factors that are thought to influence SASM location and strength are: Heinrich events, maxima in Southern Hemisphere summer insolation, and Northern Hemisphere ice sheet volume. Heinrich events are periods of intense wintertime cooling in the Northern Hemisphere that drive the SASM southwards and thus increase precipitation in the Altiplano. Paradoxically, this cooling of the Northern Hemisphere is actually due to increased iceberg and meltwater discharge. The input of larger levels of freshwater into the North Atlantic ocean leads to a marked decrease in salinity, causing changes in ocean circulation that can influence monsoon intensity (Bender, 2013). The cooling of the Northern Hemisphere changes the thermal gradient between the Northern and Southern Hemispheres, forcing the SASM to develop further south and thus increasing its strength over the 15°-22°S Altiplano (Garreaud et al., 2003). Another proposed forcer of SASM strength in the Altiplano is Southern Hemisphere summer insolation – that is, the amount of incident solar radiation onto the Southern Hemisphere. The seasonality of insolation over an area varies cyclically over a period of 19 ka & 23 ka due to Earth's precession, as well as on longer timescales due to other Milankovitch forcings (Mohtadi et al., 2016). Highs in austral summer insolation increase the heating of the Southern Hemisphere continents, driving monsoons southwards and leading to greater precipitation over the Altiplano (Mohtadi et al., 2016). Finally, the Laurentide ice sheet during the last glacial maximum (LGM) considerably altered the relief of much of North America, and so significantly affects

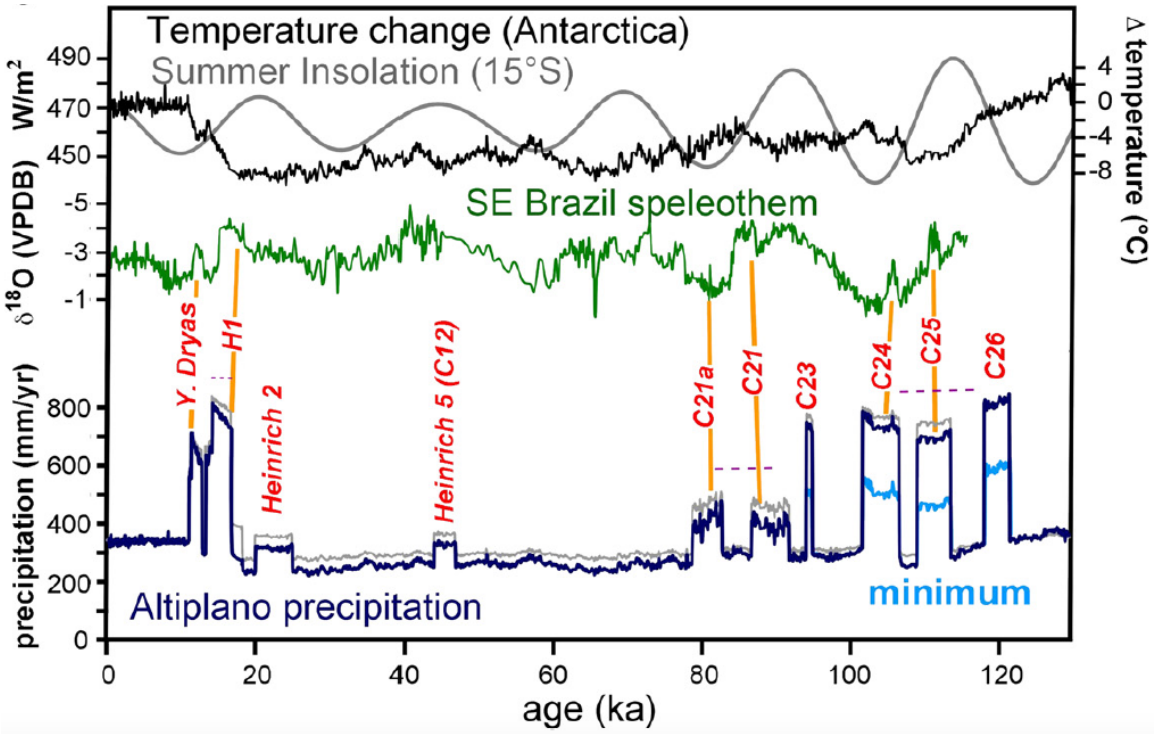

Figure 1-2: Plot of temperature change, summer insolation, speleothem δ^{18}O (as a proxy for SASM intensity) (Cruz et al., 2005) and modelled precipitation of the Altiplano over the past 130 ka. The modelled precipitation shows clear, abrupt shifts to higher rainfall during Heinrich events and earlier, analogous Northern Hemisphere cooling events (C21a-C26). However, the Heinrich events that indicate increased precipitation often coincide with high summer insolation, and do not all show a marked increase in SASM strength in the speleothem record. Figure originally from Placzek et al. (2013).

air circulation throughout the Americas (Pausata et al., 2011), which could also be responsible for forcing the SASM southwards and increasing Altiplano rainfall. As shown in Figure 1-2, these events often coincide, making their respective impacts difficult to disentangle.

1.2 Current Lake Level Reconstruction Challenges

While the overarching goal of paleolake level reconstructions in this region is to better understand the climatic factors that force the SASM, significant barriers remain before lake level reconstructions are robust enough to resolve this issue. The size of the lake basins being studied, difficulties in geochronology in the region, and a lack of scientific

consensus surrounding highstands before 20 ka all need to be addressed before we can better understand past water availability in the region.

Before the last deglaciation, significant uncertainty remains around the timing of these lake highstands. One common method for studying lake level variations is dating material within sediment cores that provide a continuous record from which to constrain the ages of wet versus dry periods within the basin. However, applying geochronological tools to sediment cores is difficult as they often lack appreciable amounts of quality datable material (Chen et al., 2019). For example, when dating sediment cores from the Titicaca-Uyuni lake system, the age of one halite sample was calculated as approximately 59 ka using U/Th dating (Fritz et al., 2004) and approximately 191 ka using Argon dating (Fornari et al., 2001). While this discrepancy is an extreme case, it serves as an important example of the lack of well-constrained geochronology in this area. U/Th and radiocarbon dating of bath-tub carbonate deposits is generally a more reliable geochronological tool, however, these individual tufa deposits are not continuous, and therefore do not represent a complete record of hydrology within these basins. In order to resolve SASM forcing parameters, it will also be important to precisely date continuous lake level markers to determine if the

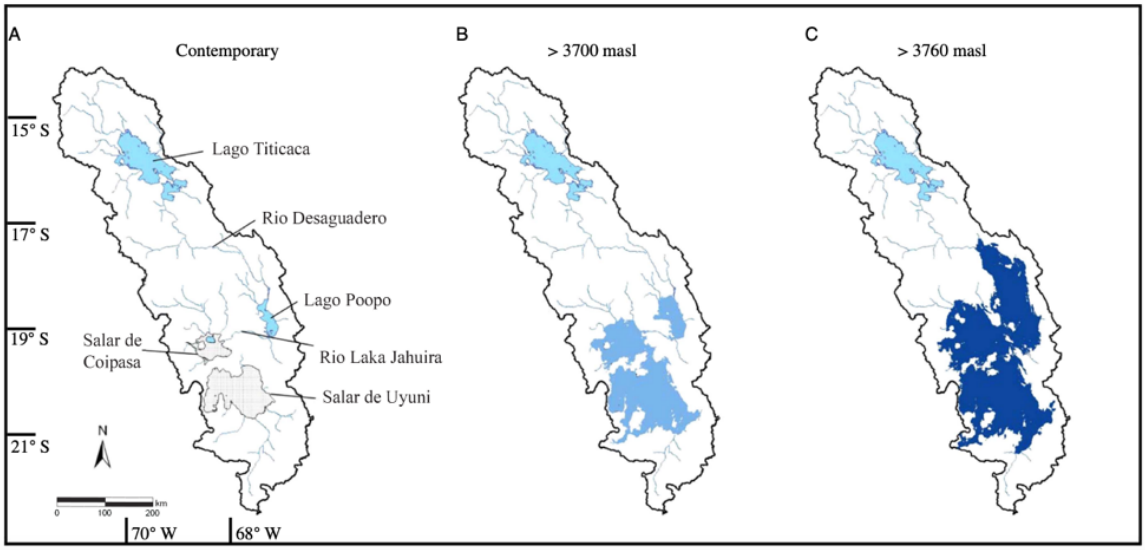

Figure 1-3: Map of the Titicaca-Uyuni basin, illustrating the continuous lake system spanning over 6° of latitude when lake levels rose to 3760 meters above sea level during the last deglaciation.

timing of forcing events clearly corresponds with highs in lake level.

Furthermore, even when general scientific consensus supports the presence of a lake level highstand during the last deglaciation, the lake basin studied is too large to properly constrain latitudinal variations in the SASM. As shown in Figure 1-3C, when Altiplano lake levels reach 3760 m above sea level, the individual basins of Uyuni, Coipasa and Poopo form one extended lake system that is connected to the Titicaca basin (Nunnery et al., 2019). This means that the large Titicaca-Uyuni basin being studied in current literature (Baker & Fritz, 2015; Nunnery et al., 2019; Placzek et al., 2006) does not constrain SASM precipitation location closely, as this system spans approximately 6° of latitude. As an extreme example, during the last deglaciation it is possible that SASM precipitation amount only increased between 15°-17°S, and yet this signal is observed at 21°S due to the extensive nature of this basin. In order to better understand past SASM changes, a smaller hydrologically closed basin should be studied to more tightly constrain the latitude at which precipitation amount changes.

Finally, there are significant debates regarding the interpretation of carbonate data suggesting a lake level highstand between 120-100 ka. As shown in Figure 1-1, lake level reconstructions from the Poopo basin (which have been extrapolated across the Titicaca-Uyuni basin) suggest a highstand occurred at around 3720 meters above sea level between 120-100 ka (Placzek et al., 2006). This lake level elevation would correspond to a lake system somewhere in between the Figure 1-3B & 1-3C scenarios. Placzek et al. suggest that at this elevation the Poopo, Uyuni and Coipasa basins would form a continuous lake system, even though carbonate deposits at this elevation have not been identified in the Uyuni or Coipasa basins (Placzek et al., 2013). However, Baker & Fritz argue that sediment core records from the Salar de Uyuni do not indicate an active lake system at this time, and suggest that only the Poopo basin experienced elevated lake levels (Baker and Fritz, 2015). Understanding if this 120-100 ka lake level highstand was contained within the Poopo basin, or extended into the Uyuni and Coipasa basins, has important implications for the latitude of SASM precipitation during this period. Therefore, examining if increased precipitation occurred over the more southerly portion of the Titicaca-Uyuni basin

will be necessary to understand how to interpret this lake level highstand.

1.3 The Salar del Huasco – Why Here?

The Salar del Huasco is a hydrologically closed basin within the northern Chilean section of the South American Altiplano, at an elevation of 3800 m above sea level and a latitude from 20.2-20.3°S (Hernández et al., 2016). Precipitation at Salar del Huasco occurs entirely during the SASM (Hernández et al., 2016) and is currently low, as the vast majority of SASM precipitation occurs further north. Surface runoff during the monsoon, and groundwater aquifers that are refilled seasonally by the SASM, are the only water sources contributing to the shallow wetland system (Hernández et al., 2016). During the SASM streams carry water into the Salar del Huasco from nearby groundwater sources, forming ponds. As the water table drops in the following months, these stream systems dry up and these ponds become isolated due to evaporation, which is the only means of water loss from the hydrological system (Johnson et al., 2010).

Figure 1-4: Map of a portion of the Altiplano, highlighting the Uyuni and Huasco basins and their similar latitude. The Salar del Huasco is outlined in blue (representing the maximum elevation of past lakeshores). The red circular marker indicates the sample collection point for this thesis.

As shown in Figure 1-4, the Salar del Huasco exists at a similar latitude to the much larger Salar de Uyuni system, but is in a discrete drainage basin. The similar site latitudes mean that similar precipitation patterns are expected between the two basins. The Salar del Huasco lake level chronology can therefore act as a control to verify if we see similar dates for lake level maxima between the Uyuni and Huasco basins. Furthermore, the smaller size of the Huasco drainage basin means that lake level highs must correspond to the balance of precipitation and evaporation at that latitude, whereas the far greater latitudinal range of the Titicaca-Uyuni lake system – which spans over 6° of latitude during highstands (Nunnery et al., 2019) – could be fed by SASM precipitation significantly further north. As the Titicaca-Uyuni drainage system has been studied in much more detail (Placzek et al., 2013), the Salar del Huasco tufas offer an opportunity to independently verify what the precipitation variations in the Altiplano at 20.2-20.3°S have been throughout time.

In order to create a lake level chronology for the Huasco basin, paleo-lakeshore carbonates deposited at known elevations above the modern flat were studied. These tufas – carbonate deposits often associated with microbial activity (Pedley et al., 2009) – form near the shoreline of lakes, and therefore indicate lake level variations through time. By creating a lake level chronology, we can compare the timing of lake level highstands to those in neighboring basins, and begin to determine the synchronicity of the Huasco and larger Altiplano basins.

As well as being sourced from an understudied drainage system, the tufas studied in this report are unique in that each sample represents extended periods of lake history. Rather than a single, fairly homogenized carbonate sample, some Salar del Huasco tufas form highly unusual thinly laminated carbonate layers corresponding to discrete depositional periods, similar to speleothem growth patterns. This means that a single sample spans a substantial range of time and may even record multiple lake highstands. Studying these samples has the potential to alleviate a significant previous issue – that is, that paleolake shore data are often skewed towards more recent time intervals because the sampling of lakeshore carbonate deposits becomes increasingly difficult the further back in time one wishes to study. This difficulty in

finding older tufas to study is reflected in Figure 1-1, which illustrates the uneven time period sampling that is skewed towards the past 20 ka. In addition, Salar del Huasco tufas form a continuous record, which can be dated well and has a geologic context unambiguously related to past lake levels. This is in contrast to other more common geologic lake level indicators used in previous literature (Baker & Fritz, 2015), such as traditional carbonates, which can be dated well but are not continuous, or lake sediment cores which are continuous but difficult to date. Speleothem oxygen isotope records are both continuous and reasonably dateable but can be influenced by many factors besides local precipitation amount, which are difficult to disentangle. Therefore, by studying these types of previously unknown multi-layer tufas, earlier dates may be resolved from fewer samples, decreasing the number of tufa deposits necessary to form a lake level chronology.

1.4 Principles and Benefits of U/Th Dating

The Salar del Huasco tufas were dated using uranium/thorium dating in lab. Put simply, the essential principle behind U/Th dating is that uranium is soluble in water, whereas thorium-230 (its daughter isotope) is highly insoluble in water with pH > 3 (Chen et al., 2019; Schwarcz, 1989). Therefore, when tufa carbonates precipitate, they preserve this high fractionation between uranium-238, uranium-234, and thorium-230. Over time as both uranium-238 and uranium-234 decay, the amount of thorium-230 within the tufa carbonate will increase, and by comparing these values and their approach to secular equilibrium with uranium-238, we can determine the age of the tufa sample.

In order for U/Th dating techniques to be applied with confidence, there are fundamental requirements for the carbonate samples we study. Firstly, the U-series decay system within the carbonate must have remained closed after deposition – that is, no post depositional leaching or addition of U or Th isotopes can have occurred. Secondly, there must have been an absence of thorium-230 within the precipitated carbonate initially, or this initial thorium-230 must be able to be accurately corrected

for. The extent to which this condition is met can be estimated by measuring thorium-232, which is a long-lived isotope (half-life ∼14 Ga) over the timescales we apply U/Th dating (Chen et al., 2019), and is expected to have similar fractionation in water to thorium-230. Therefore, if high amounts of detrital thorium-232 exist in our tufa samples, it is likely high initial thorium-230 was incorporated into our samples, leading to greater uncertainties when dating these tufa layers.

For this study, U/Th dating was applied rather than the more common radiocarbon dating method for several reasons. Firstly, as discussed above, current lake level chronologies are biased towards younger time periods. ^{14}C dating has an upper limit for reliable dating of around 45 ca. ka (Placzek et al., 2006), whereas U/Th dating has a practical limit of around 700 ka (Chen et al., 2019). Therefore, using U/Th dating can allow us to resolve lake level highstands well before 45 ka, which may in the future be important for understanding the impacts of orbital shifts and glacial periods on SASM strength and location over long time periods. In addition, radiocarbon dating of lake carbonates can be impacted by both contamination by younger carbon (e.g. from secondary organic matter or modern CO_2 incorporation), leading to age estimates that are too low, or by lake reservoir effects in which lakes are depleted in ^{14}C and so yield age estimates that are too high (Placzek et al., 2006). Altiplano lakes commonly have ^{14}C reservoir effects of several thousand years (Geyh et al., 1999). To avoid these potential sources of error, and to be able to study lake level highstands older than 45 ca. ka, U/Th disequilibrium dating was applied.

Chapter 2

Methods

2.1 Sample Collection

The samples studied were collected from the Salar del Huasco basin in 2016 by Dr. Christine Y. Chen, a former graduate student in the McGee Lab. Fieldwork was conducted over two days. All samples were collected from one location in the basin: a basaltic hill approximately 20 meters tall surrounded by salt flats. Sample elevations varied within this one collection location, and were measured with a Trimble Geo7x differential GPS device, which can measure vertical elevations to within $\pm$ 1 m precision (2σ level). Three samples that displayed the unusual laminated depositional pattern (discussed in Introduction Section 1.3) were studied intensively: CYC16-061, CYC16-062 and CYC16-064. A further three samples (CYC16-066B, CYC16-067 and CYC16-071) had preliminary work done.

2.2 Sample Processing and Drilling

For all samples within this thesis, the following naming convention will be used:

CYC16-000A(Z)

Here, CYC16 indicates that these tufa samples were collected by Christine Y. Chen in 2016. "000" is the identifying sample number. "A" or "B", which sometimes

immediately follow the sample number, indicate one particular cut of a tufa sample, when multiple cuts of the same tufa are discussed within this work and need to be differentiated. "(Z)" refers to a particular U/Th hole and/or corresponding powder that was drilled from that tufa sample.

Samples were cut with a rock saw and polished with diamond stone buffers in the following descending grit size: 3000, 1500, 800, 400, 200, 100, 50.

U/Th and stable isotope powders were then drilled from the cut samples, using 0.8 mm and 0.5 mm drill bits respectively. Drill bits were cleaned with dilute HCl and methanol between every drill hole. Depending on mass spectrometer sensitivity and 238U concentration of the specific sample, between 20-30 mg of each powder sample were needed for U/Th dating. Stable isotope drill hole lines were oriented parallel to the growth plane of the tufas, and spaced 1.42 mm apart for samples CYC16-061A, CYC16-062 and CYC16-064. Between 1-2 mg of powder was drilled for each stable isotope measurement. Samples CYC16-071A, CYC16-066B and CYC16-067 were randomly drilled for stable isotope powders a total of 12, 5 and 10 times respectively.

2.3 Uranium/Thorium Chemistry

The drilled powder sample was added to a 22 mL Teflon beaker and combined with 1 mL of MilliQ (MQ) water, 3 drops of 16N nitric acid and 1 mL of 8N nitric acid. A gravimetrically calibrated ^{229}Th-^{233}U-^{236}U spike was then added to achieve a 2:1 ratio of ^{235}U:^{236}U. 10 drops of hydrogen peroxide were added, and the solution was refluxed on a hot plate at approximately 110°C for 1 hour. After this the solution was uncapped and dried down at approximately 125°C.

The sample was then redissolved into 1 mL of 6N hydrochloric acid and transferred into a centrifuge tube. The beaker was rinsed with MQ water and this rinse was added into the centrifuge tube and diluted further with MQ water until total solution volume in each tube was 10 mL. 7 drops of Fe solution were added, and NH_4OH was added dropwise until Fe oxyhydroxides began to precipitate out. The solution was then centrifuged for 5 minutes at 3000 rpm, the supernatant was discarded and

MQ water was re-added up to 10 mL and centrifuged again. The supernatant was again discarded and the sample was redissolved in 1 mL of 8N nitric acid before being transferred to a clean beaker and dried down at 120°C. 2 drops of 16N nitric acid were added and dried down at 120°C. The sample was redissolved in 0.2 mL 8N nitric.

Columns were loaded with 200-400 mesh AG1X8 resin, and washed with 1.5 mL MQ water and 1 drop of 16N nitric acid. It was subsequently washed with 1 mL 8N nitric acid and 0.5 mL 8N nitric acid, being allowed to drain fully. The sample was added to the column and washed with 1 mL and then 0.5 mL of 8N nitric acid. Thorium was then collected in a separate beaker by eluting with 1 mL of 6N hydrochloric acid followed by 0.5 mL of 6N hydrochloric acid. Finally, uranium was collected in a separate beaker by elution with 1 mL of MQ water twice.

10 drops of hydrogen peroxide were added to each sample and dried down at approximately 95°C. This was repeated. 3 drops of 16N nitric acid were added and dried down until only a tiny drop remained, then another drop of 16N nitric acid was added and dried down until a tiny drop remained. The uranium and thorium fractions were separately redissolved in 2% nitric acid, at an appropriate concentration for MS measurements. Uranium and thorium fractions were run on a Nu Plasma II-ES MC-ICP-MS, and an initial $^{230}Th/^{232}Th$ ratio of 4 ± 3.5 ppm was assumed for the age calculations of all samples.

2.4 Stable Isotope Measurements

The drilled stable isotope powders were processed and measured in the Environmental Isotope Laboratory at the University of Arizona.

2.5 Replicate Ages

All tufa samples studied had at least two depths at which replicate U/Th dates were produced. These replicate dates were combined into a single error-weighted mean age and a weighted mean 2σ standard deviation or a mean squared weighted deviation

(MSWD) (Ludwig, 2003; Wendt and Carl, 1991). To be conservative, whichever standard deviation was larger was used, even when the MSWD calculation suggested the data was under-dispersed. To calculate the weight of each element:

$$w_i = \frac{1}{\sigma_i^2} \tag{2.1}$$

To calculate the weighted mean, where n is the total number of replicates:

$$\bar{x} = \frac{\Sigma_{i=1}^{n} w_i x_i}{\Sigma_{i=1}^{n} w_i} \tag{2.2}$$

To calculate the weighted mean standard deviation:

$$\sigma_{\bar{x}} = \sqrt{\frac{1}{\Sigma_{i=1}^{n} w_i}} \tag{2.3}$$

To calculate the MSWD:

$$MSWD = \frac{1}{n-1}\left[\Sigma_{i=1}^{n} \frac{(x_i - \bar{x})^2}{\sigma_i^2}\right] \tag{2.4}$$

Now use the MSWD to correct for over- or under-dispersion of the data:

$$\sigma_{MSWD,i} = \sigma_i \times \sqrt{MSWD} \tag{2.5}$$

To calculate the MSWD-adjusted weights:

$$w_{MSWD,i} = \frac{1}{\sigma_{MSWD,i}^2} \tag{2.6}$$

Finally, calculate the weighted mean MSWD-adjusted standard deviation:

$$\sigma_M = \sqrt{\frac{1}{\Sigma_{i=1}^{n} w_{MSWD,i}}} \tag{2.7}$$

The standard deviation used was whichever standard deviation was largest, $\sigma_{\bar{x}}$ or σ_M.

2.6 Constructing Proxy Records from Age models (COPRA)

Discrete U/Th ages generated along the depth of each of the samples CYC16-061B, CYC16-062 and CYC16-064 were linearly interpolated along the length of the sample using COPRA modelling to provide a continuous age-depth model for each sample (Breitenbach et al., 2012). This age-depth model was used to assign ages to the stable isotope drill holes that were drilled at set depth intervals along each sample.

For CYC16-061B, drill holes G & M defied stratigraphic order and so were excluded from the COPRA age-depth model. The depth (from the sample top) of the apparent hiatus in CYC16-061B (31.3165 mm) was input into COPRA, and two different age Monte-Carlo Age simulations were run for the older and younger sample portions. CYC16-062 and CYC16-064 both contained tractable age reversals, but were within σ uncertainty so were not excluded. Two thousand Monte-Carlo simulations were run for each sample.

Chapter 3

Results

3.1 Sample Collection and Processing

Table 3.1: Elevation data, and information on types of analyses applied to the samples.

Sample Name	Elevation	U/Th Dated?	Stable Isotope
CYC16-061	3819.0 ± 0.9	Y	Y
CYC16-062	3819.5 ± 0.8	Y	Y
CYC16-064	3809.0 ± 0.8	Y	Y
CYC16-066	- -	N	Y
CYC16-067	3802.5 ± 0.8	N	Y
CYC16-071	3819.1 ± 0.8	N	Y

Table 3.1 and Figure 3-1 show the sampling site of Salar del Huasco, and give an overview of sample elevation information and the types of analyses (U/Th dating and/or stable isotope measurements) conducted on each of the samples.

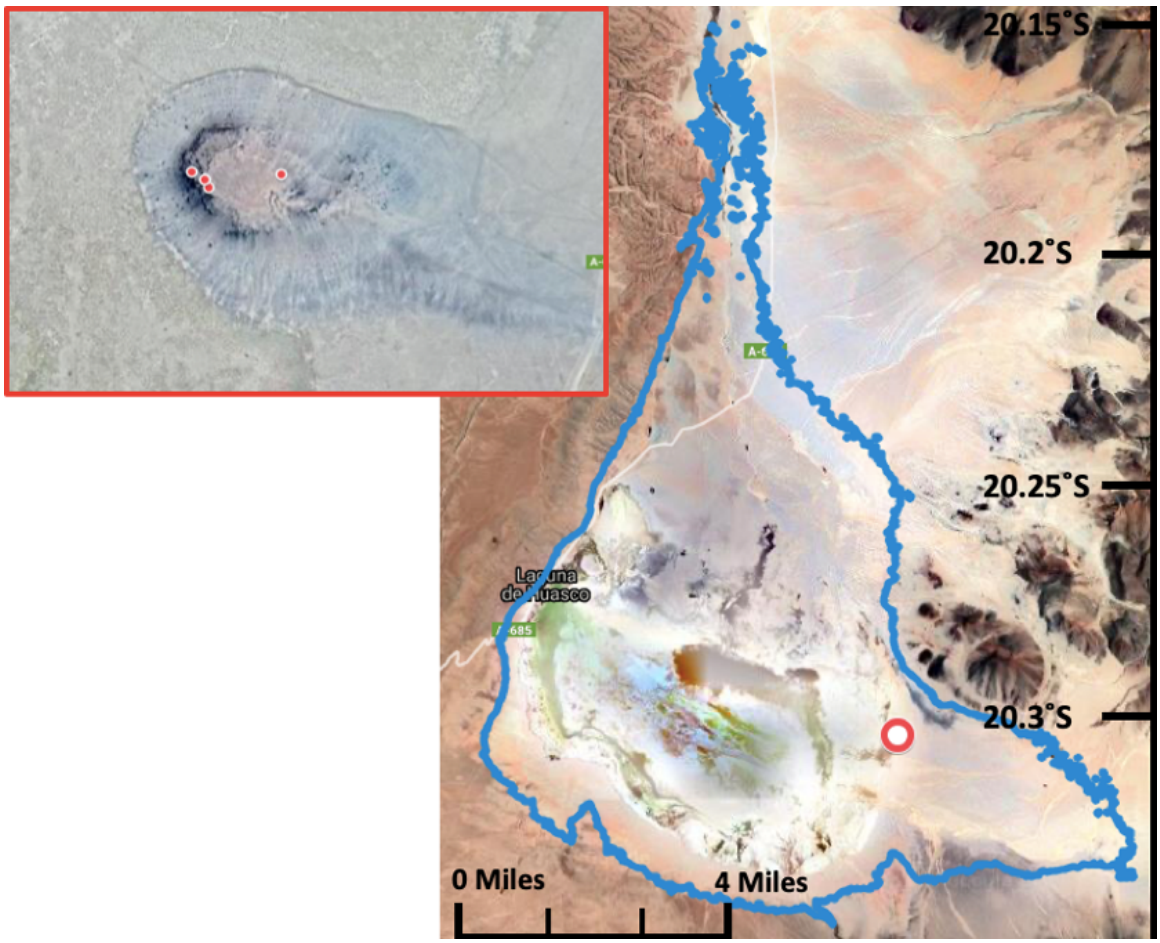

Figure 3-1: Map of the Salar del Huasco with the lake level maximum boundary drawn in blue. Red rectangle shows the sampling site in detail, with the 6 samples discussed in this report all having been collected from this basalt feature at different elevations. Lake level outline courtesy of research by AJ Iversen.

In Figures 3-2 to 3-4, holes drilled for stable isotope powders are labeled in blue. Holes drilled for U/Th dating are labeled in red. Holes that contributed to a replicate age measurement are denoted as X_Z, where X represents the name of the hole and Z represents its corresponding replicate hole. A ruler in millimeters is shown on the right of each of the sample scans for scale.

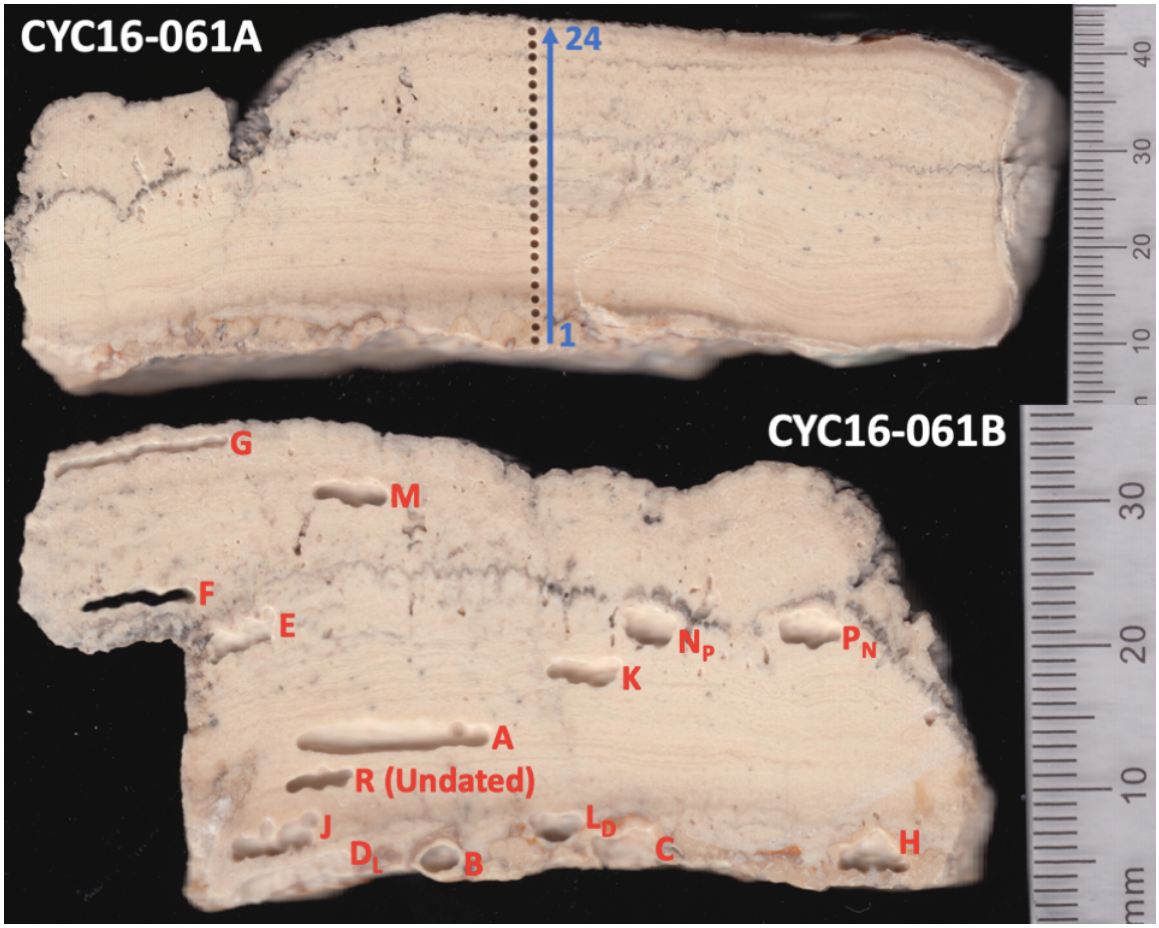

Figure 3-2: Compiled scans of sample CYC16-061A and CYC16-061B. Stable isotope powders were drilled from CYC16-061A, while U/Th powders were drilled from CYC16-061B. Stable isotope powders were numbered from 1-24 along the growth plane of the tufa. U/Th powders spanned from A-R, omitting I and O. Replicates of the same tufa layer were: D & L, N & P.

Figure 3-2 shows the stable isotope and U/Th drill holes for samples CYC16-061A and CYC16-061B. These samples are different cuts of the same tufa sample. The age versus depth data generated from CYC16-061B was superimposed on CYC16-061A to create a stable isotope vs age plot in COPRA. CYC16-061B(R) was drilled for U/Th dating but was unable to be dated due to lab closure.

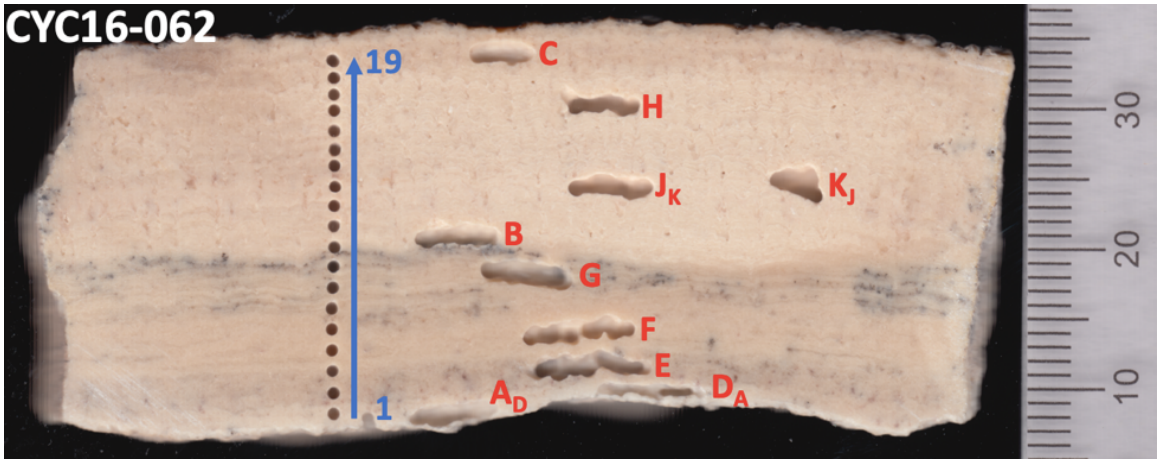

Figure 3-3: Compiled scans of sample CYC16-062. Stable isotope powders were numbered from 1-19 along the growth plane of the tufa. U/Th powders spanned from A-K, omitting I. Replicates of the same tufa layer were: A & D, J & K.

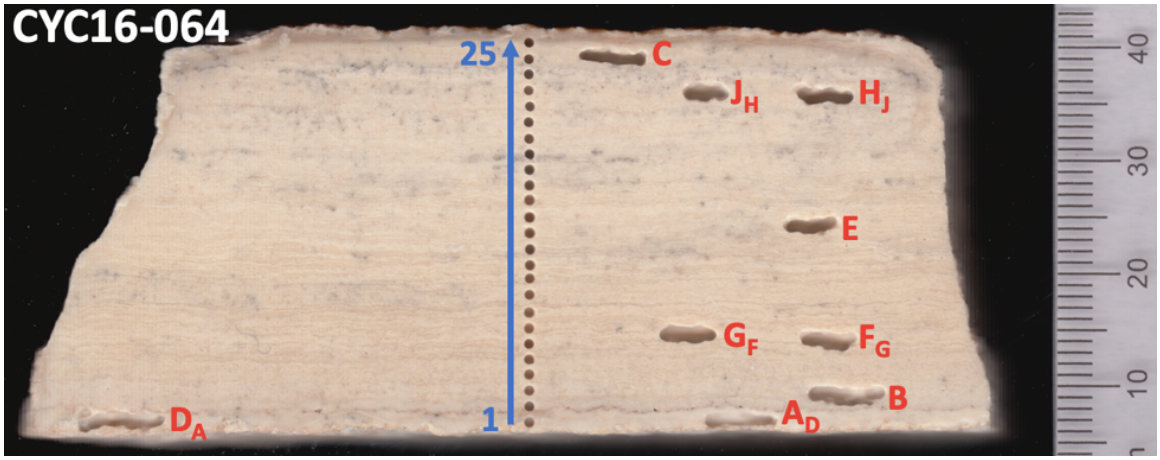

Figure 3-4: Compiled scans of sample CYC16-064. Stable isotope powders were numbered from 1-25 along the growth plane of the tufa. U/Th powders spanned from A-J, omitting I. Replicates of the same tufa layer were: A & D, F & G, H & J.

Figures 3-3 and 3-4 show the U/Th and stable isotope drill holes for samples CYC16-062 and CYC16-064, respectively. For each of these samples, depths were interpolated onto the stable isotope drill axis for all final depth comparisons. As CYC16-062 was significantly less linear than CYC16-064, the uncertainties in making this translation will be greater for CYC16-062 than CYC16-064.

3.2 U/Th Dating Results

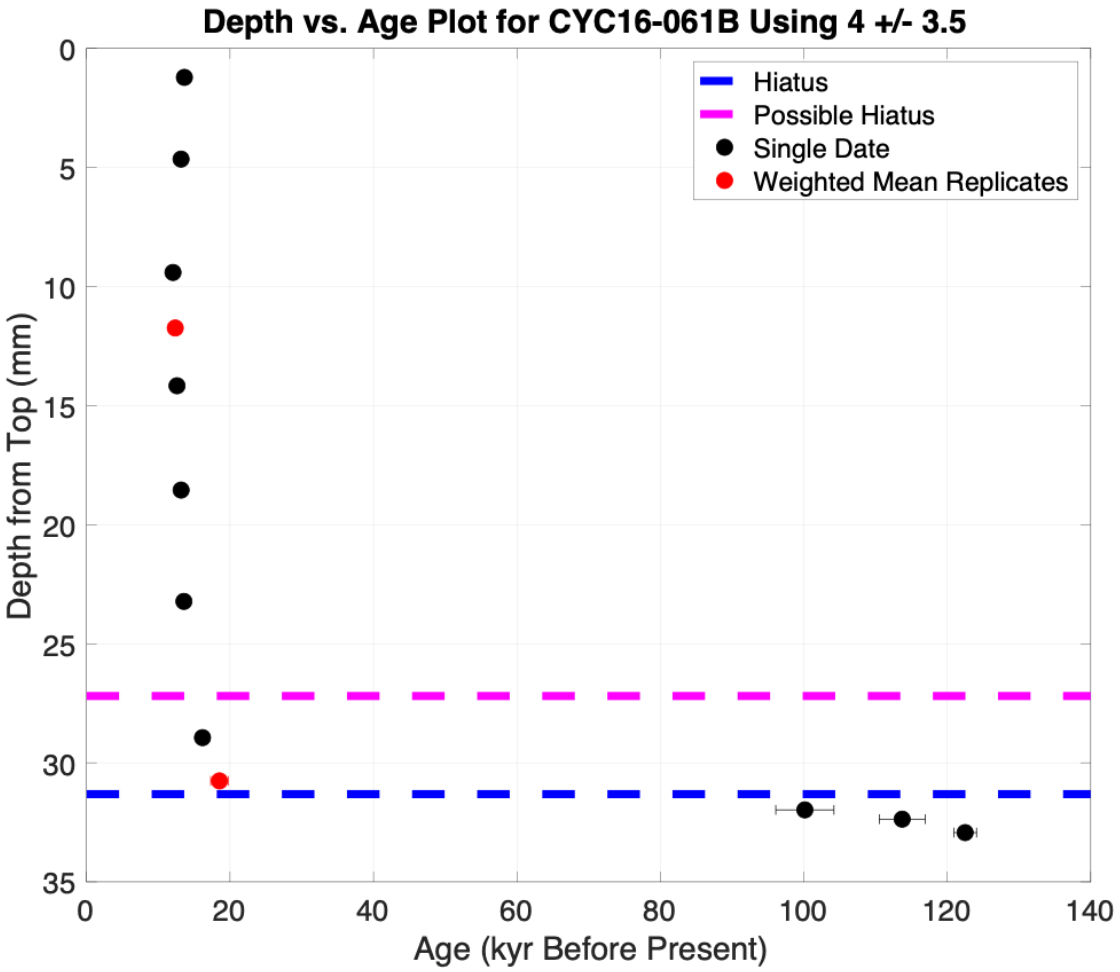

Figure 3-5: Complete depth vs age plot for CYC16-061B. Depositional hiatus shown in blue. Possible depositional hiatus which has not yet been investigated shown in pink. Dates generated from a single powder are shown in black, while dates generated from weighted mean replicates are shown in red. "Using 4 ± 3.5" refers to the initial ^{230}Th / ^{232}Th ratio and its corresponding uncertainty used in the age calculations.

Figures 3-5 and 3-6 show the complete and partial (last 20 ka) depth versus age results for CYC16-061B, respectively. Figure 3-5 indicates that depositional rates prior to the hiatus were far slower or more discontinuous than those following the hiatus, as 20 ka of deposition equated to approximately 3 mm of tufa material prior to the hiatus, but the following 30 mm of tufa encapsulate only the period from 20-12 ka. The older ages in Figure 3-5 have significantly larger error bars than the earlier

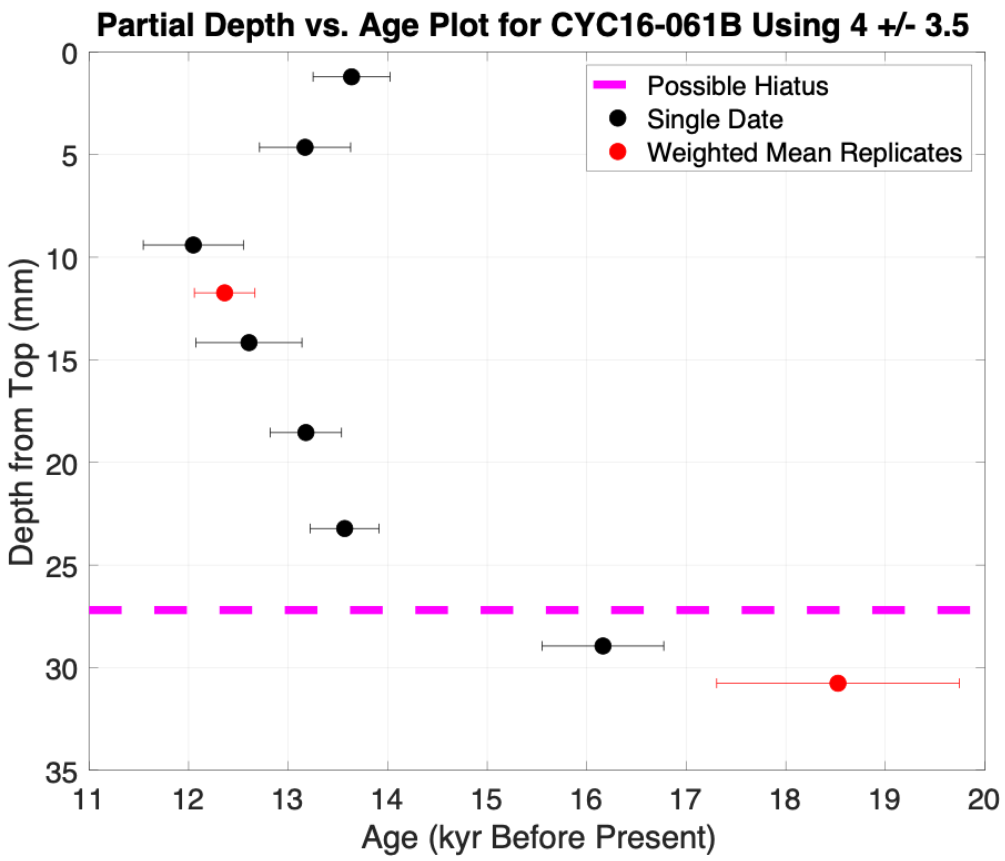

Figure 3-6: Depth vs age plot for CYC16-061B neglecting dates prior to the depositional hiatus. Possible depositional hiatus which has not yet been investigated shown in pink. Dates generated from a single powder are shown in black, while dates generated from weighted mean replicates are shown in red. "Using 4 ± 3.5" refers to the initial ^{230}Th / ^{232}Th ratio and its corresponding uncertainty used in the age calculations.

ages. From Figure 3-6, we can see that stratigraphic order is obeyed for the majority of the sample, but that between the third and second hole from the sample top, there is an age reversal. Because of this, the two sample ages nearest the top were discarded when COPRA age modeling was applied. The pink dashed line in Figures 3-5 and 3-6 indicates a possible depositional hiatus. Powder CYC16-061B(R) was drilled at this depth to determine if deposition stops or merely decreases in rate/becomes more discontinuous in this interval, but has not been dated at present.

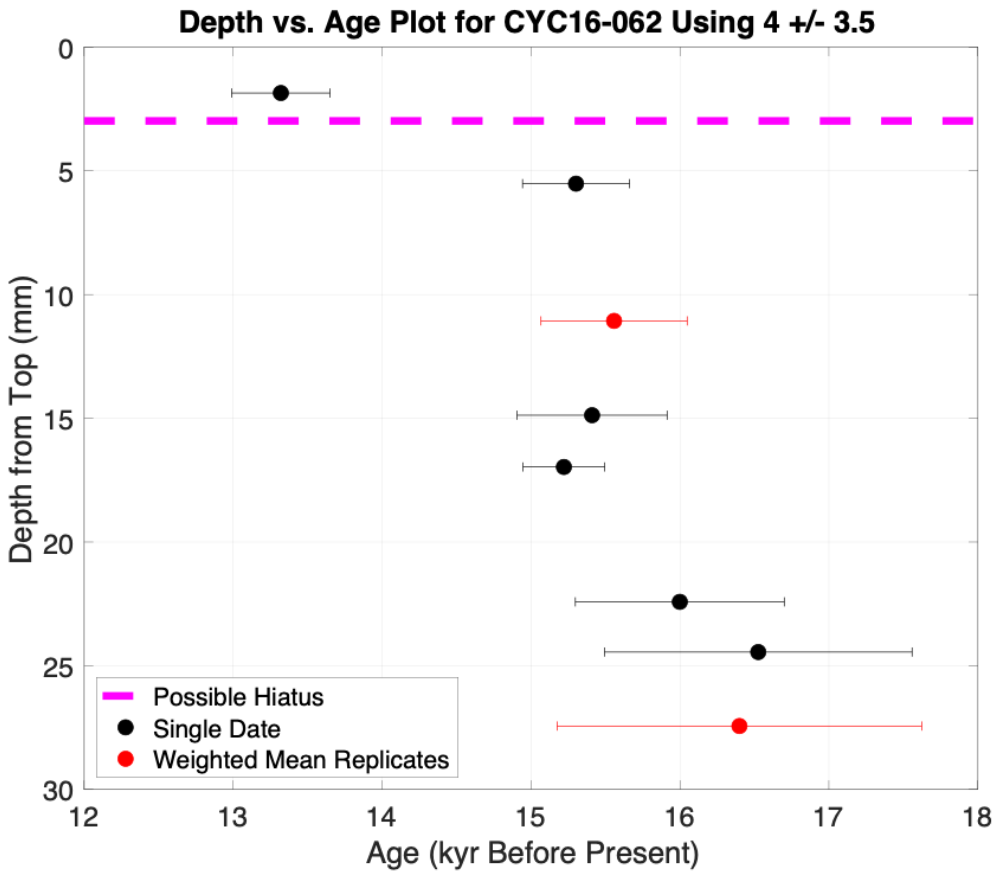

Figure 3-7: Depth vs age plot for CYC16-062. Possible depositional hiatus which has not yet been investigated shown in pink. Dates generated from a single powder are shown in black, while dates generated from weighted mean replicates are shown in red. "Using 4 ± 3.5" refers to the initial ^{230}Th / ^{232}Th ratio and its corresponding uncertainty used in the age calculations.

Similarly, Figures 3-7 and 3-8 show the age versus depth profiles of samples CYC16-062 and CYC16-064. Both of these samples had age reversals, but these reversals were within σ uncertainty and therefore not treated or removed from our age models. The majority of CYC16-062 indicates a fairly constant deposition through time between 17-15 ka, while the top age is approximately 2000 years younger than the next hole tested. This may be due to a depositional hiatus, or a decrease in rate of deposition, which is tentatively supported by a visible change in tufa color between holes CYC16-062(H) and CYC16-062(C), which span this period (see Figure 3-3). Figure 3-8 indicates that CYC16-064 shows rapid deposition between approximately

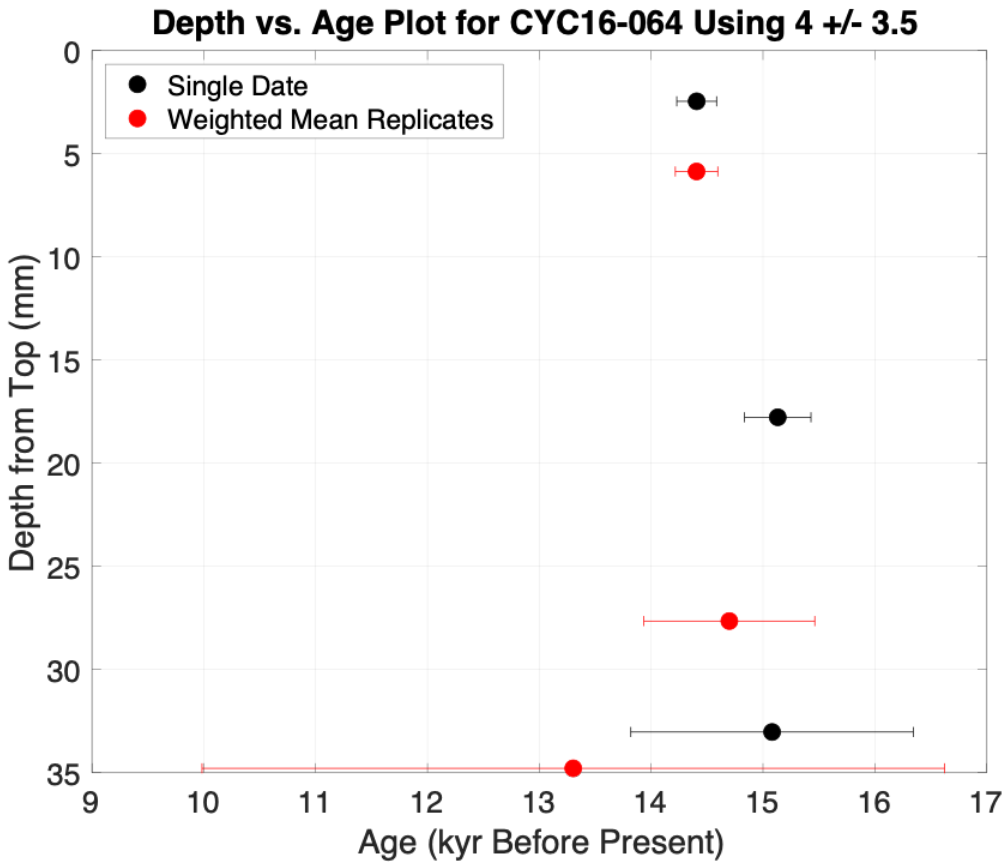

Figure 3-8: Depth vs age plot for CYC16-064. Dates generated from a single powder are shown in black, while dates generated from weighted mean replicates are shown in red. "Using 4 ± 3.5" refers to the initial ^{230}Th / ^{232}Th ratio and its corresponding uncertainty used in the age calculations.

15.5 – 14.5 ka. The powder with the greatest depth from the sample top is dated to be significantly younger than the tufa deposited later, but also has an MSWD-adjusted uncertainty of 3.3 ka (2σ). This particular tufa layer (which contains holes D & A in Figure 3-4) had detrital ^{232}Th five times greater than the rest of the tufa samples.

3.3 Stable Isotope Results

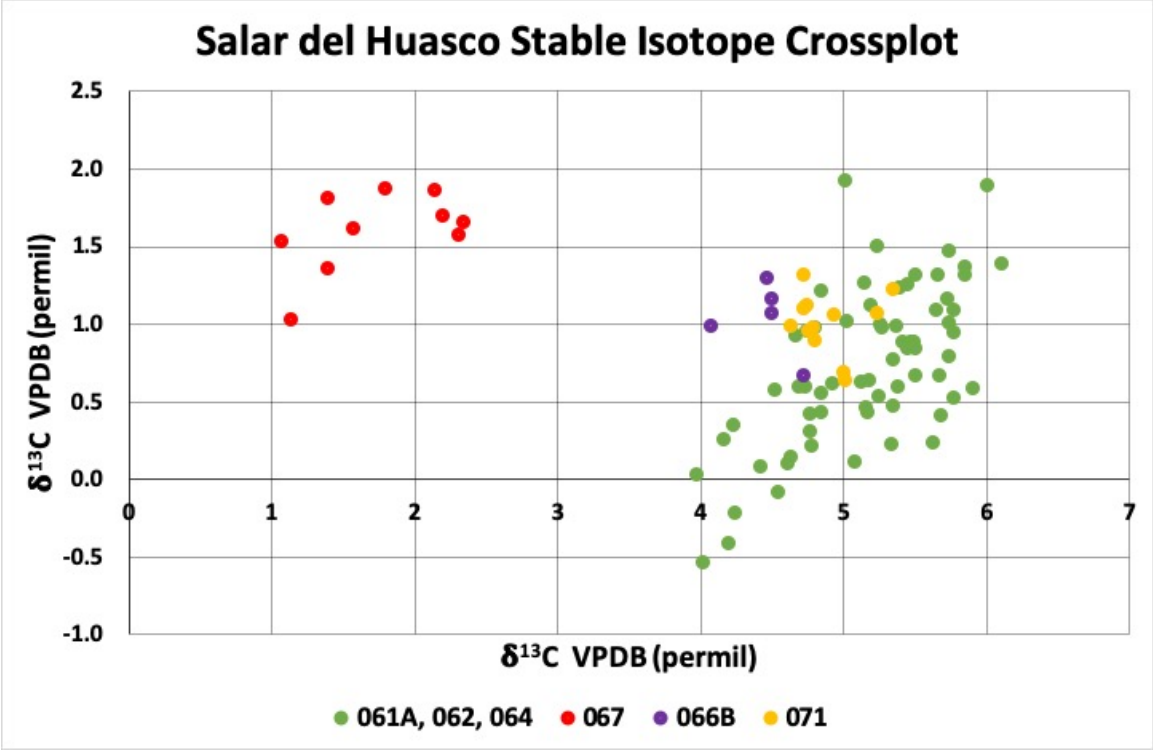

Figure 3-9: Cross plot of δ^{13}C and δ^{18}O data for samples CYC16-061A, CYC16-062, CYC16-064 are shown in green. The purple, yellow, and red data sets correspond to samples CYC16–066B, CYC16-067 and CYC16-071.

Having generated depth versus age data for our 3 key samples, stable isotope values were measured for these, along with 3 other samples from the Salar del Huasco site, to better understand variance between individual tufa samples. As seen in Figure 3-9, samples CYC16-066B and CYC16-071 fell into the same general isotope range as our key samples, whereas sample CYC16-067 had a comparable δ^{18}O but far lower δ^{13}C values. Of the six samples for which stable isotope measurements were generated, only CYC16-067 was an ikaite carbonate. Disregarding the outlying CYC16-067 values, all of the five typical tufa samples show a positive correlation between δ^{18}O and δ^{13}C data, and are enriched in both ^{13}C and ^{18}O relative to a VPDB standard. Figure 3-10 illustrates that the key samples studied all span a similar range of δ^{18}O values from -0.5 to 2 permil and δ^{13}C values from 4-6 permil.

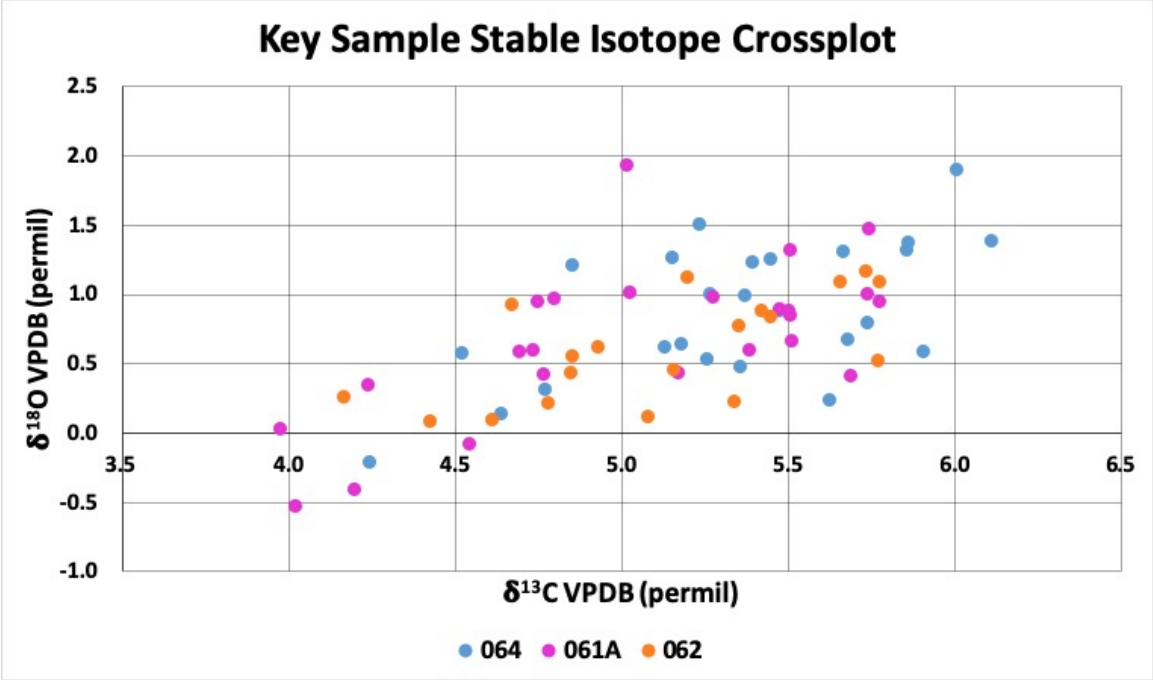

Figure 3-10: Cross plot showing key sample stable isotope values – discretized from the combined green data shown in Figure 3-9.

Stable isotope values were then plotted against a depth axis for samples CYC16-061A, CYC16-062 and CYC16-064. These samples all span a similar range of δ^{18}O and δ^{13}C values (noted in Figure 3-9), and all show positive correlation between δ^{18}O and δ^{13}C values. Interestingly, sample CYC16-064 was deposited much more rapidly than the other two samples and yet also spans the complete range of δ^{18}O and δ^{13}C values, possibly indicating an aliasing effect. δ^{18}O is substantially enriched in all of these samples when compared to local precipitation (Aravena et al., 1999).

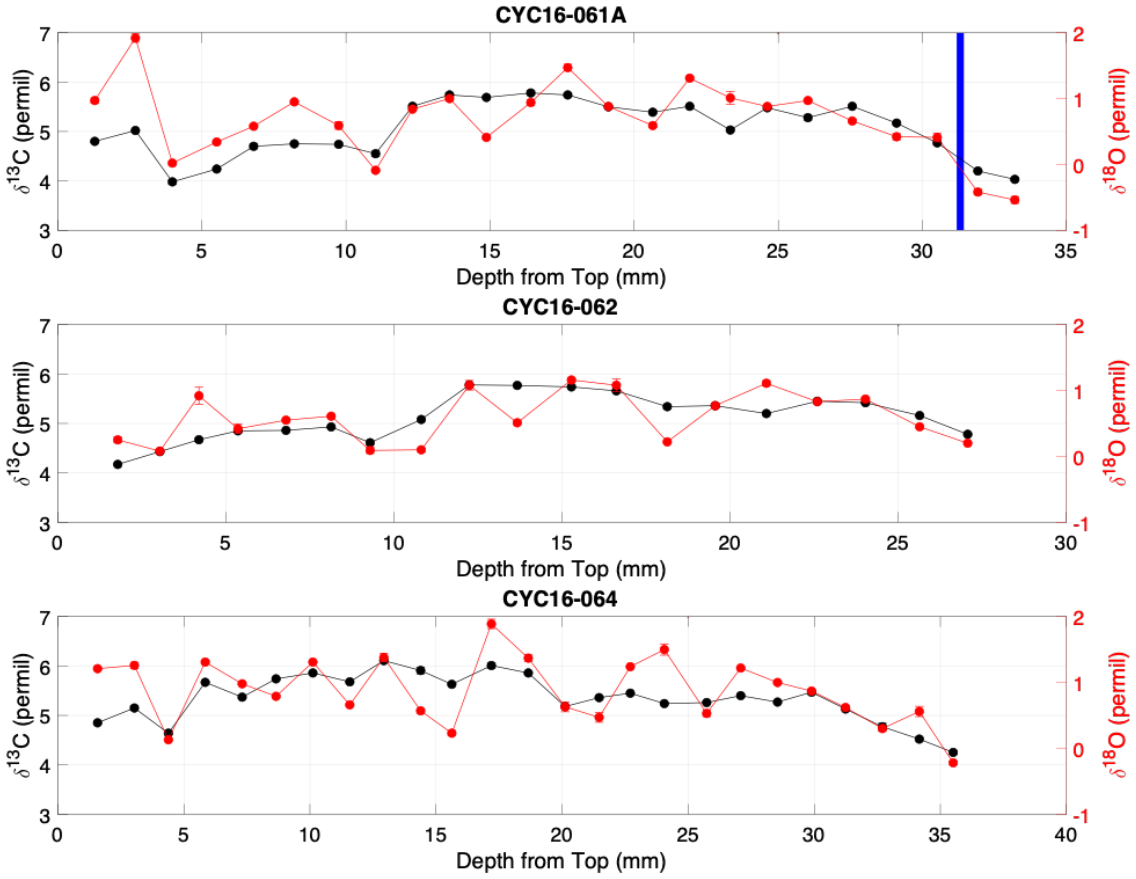

Figure 3-11: Comparison of δ^{18}O and δ^{13}C for each sample along a depth profile. δ^{18}O is shown in red while δ^{13}C is plotted in black. The known depositional hiatus in sample CYC16-061 is plotted as a blue vertical line.

The δ^{18}O and δ^{13}C values shown in Figure 3-10 were then replotted along a depth axis in Figure 3-11. All samples had reasonably strong correlation between changes in δ^{18}O and δ^{13}C values through time. Sample CYC16-061A's stable isotope values appear to diverge in the top 4 mm of the sample. δ^{18}O was more variable along the depth of the samples than δ^{13}C.

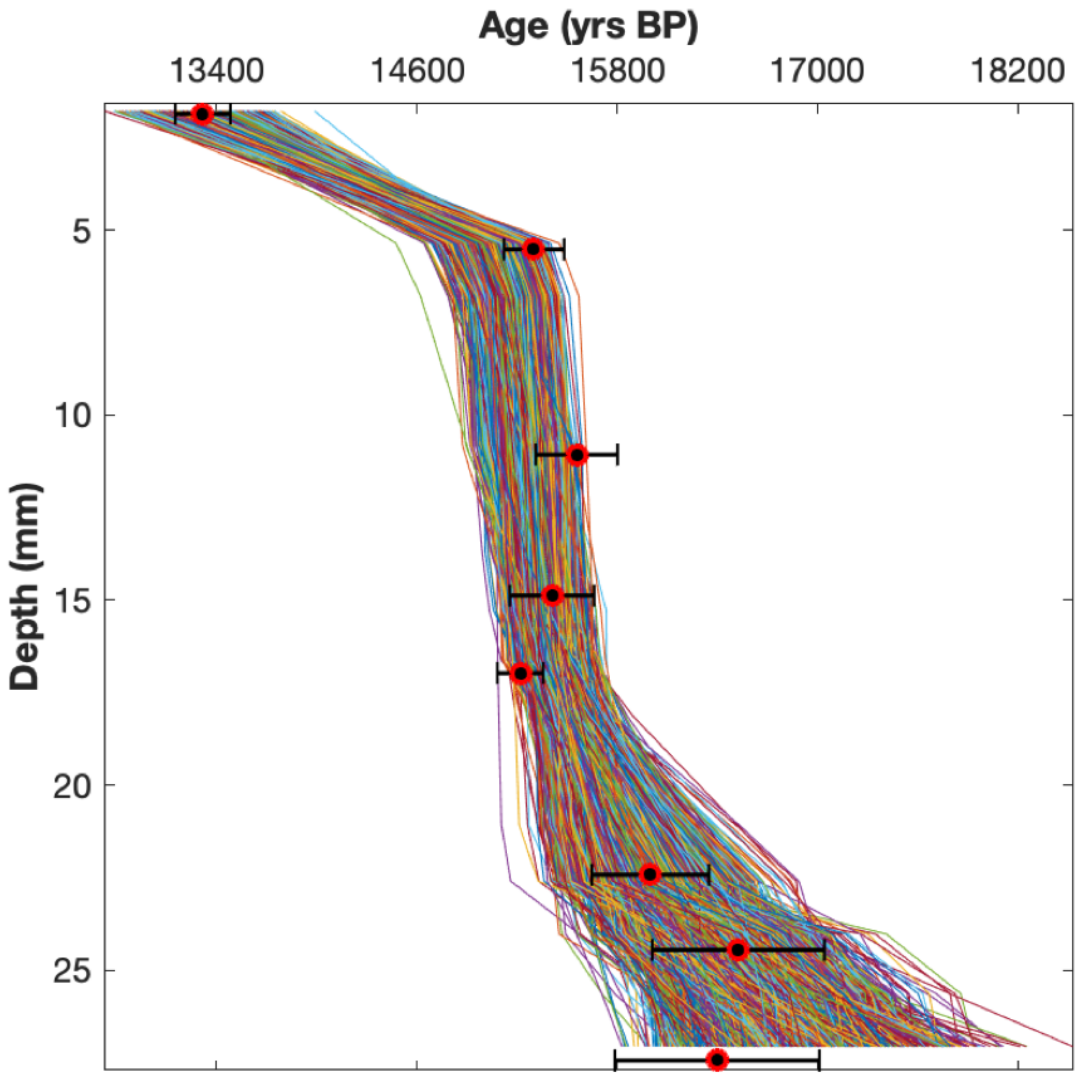

Figure 3-12: 2000 Monte-Carlo COPRA age simulations for CYC16-062. Depths and ages shown are analogous to those in Figure 3-7, but uncertainties in this model are 1σ as opposed to 2σ.

The stable isotope data versus depth shown in Figure 3-11 was uploaded into COPRA along with the depth versus age data shown in Figures 3-6 to 3-8. As an example, Figure 3-12 is a "spaghetti" plot of the 2000 Monte-Carlo simulations of the age-depth model for CYC16-062 generated by COPRA. The extent of spread between Monte-Carlo simulations at the depth extremities is typical of COPRA age models, and is also shown in the higher age uncertainties for the bottom and top (oldest and youngest) stable isotope powders in Figure 3-13.

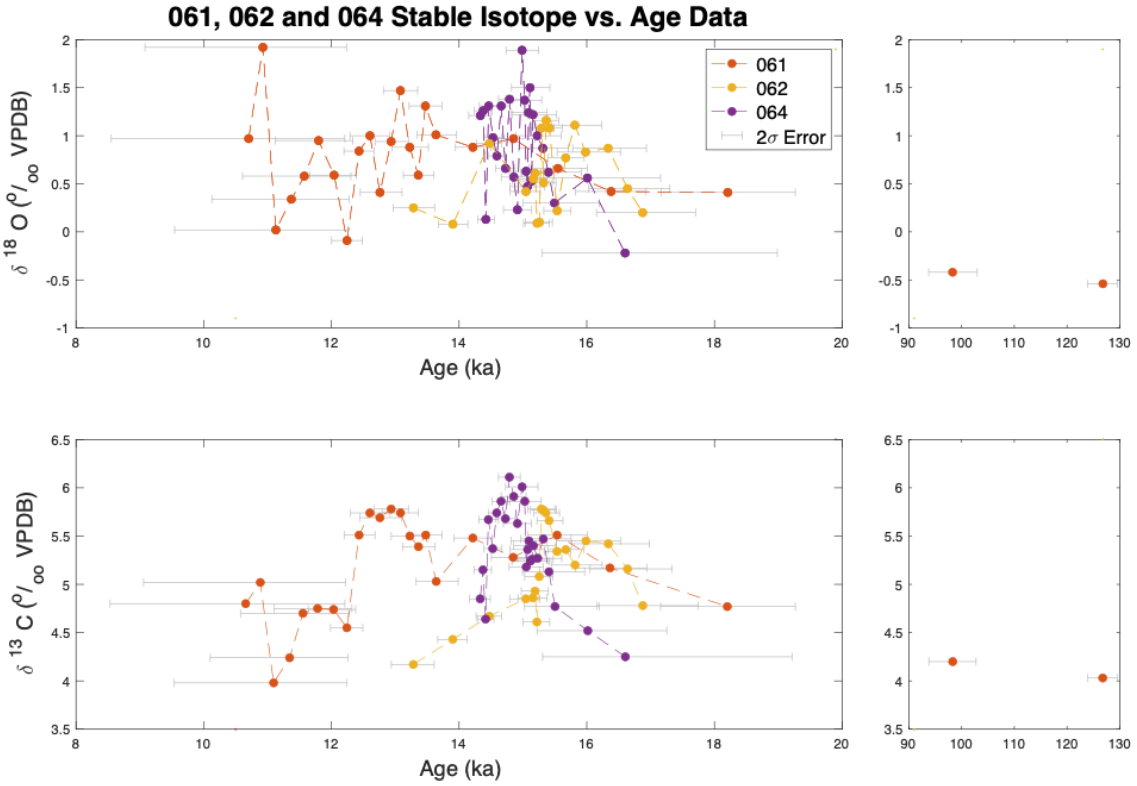

Figure 3-13: Stable isotope data plotted over time for the three samples CYC16-061, CYC16-062 and CYC16-064.

Using the interpolated age versus depth model generated by COPRA, the raw stable isotope measurements were then plotted along an age axis in Figure 3-13. Stable isotope measurements taken in the middle of the samples are more tightly constrained in age than those on the extremities. Stable isotope values from 130-90 ka are depleted in δ^{18}O and δ^{13}C when compared to the stable isotope values from the last deglaciation. Rates of deposition in each sample can be estimated by how close or separated in age each measurement was, as these measurements were taken with a fixed and consistent depth interval across all three of the samples.

3.4 Lake Level Reconstructions

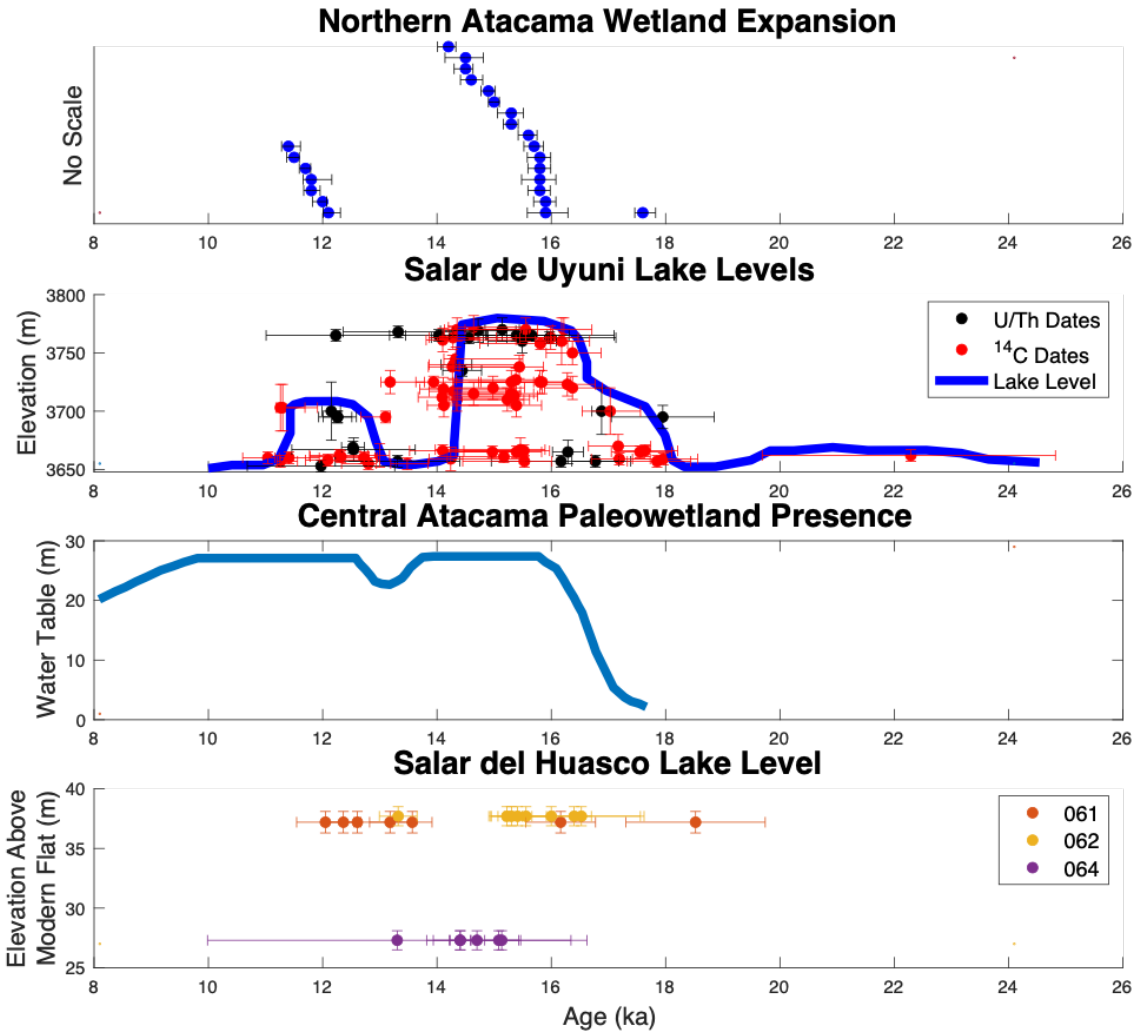

Figure 3-14: Comparison of the Salar del Huasco lake level history for the last deglaciation with other palaeohydrological reconstructions from the region by Gayo et al., 2012; Placzek et al., 2006; Quade et al., 2008. Gayo uses fossil leaf deposits as evidence for wetland expansion, Placzek dates evidence of paleo shorelines using radiocarbon and U/Th dating to reconstruct lake levels in the Uyuni basin (see Figure 1-1), and Quade dates paleo wetland sediments as evidence for wetland expansion.

Figure 3-14 compares the preliminary lake level chronology for the last deglaciation we generate from the Salar del Huasco (using ages from Figures 3-6 to 3-8 and elevation data in Table 3.1) with similar regional studies of increased water levels during this time. Broadly, our reconstruction of increased lake levels in Salar del Huasco from 18.5-12 ka agrees with the periods of increased water levels predicted

at the other sites. Our elevation record suggests a possible intermediate decrease in lake level by 10 m from 15-14 ka, which is earlier than predicted for the other sites. The dashed pink lines shown in Figures 3-6 and 3-7 indicate where the potential depositional hiatus at 37 m elevation between 15-14 ka may have occurred in samples CYC16-061B and CYC16-062.

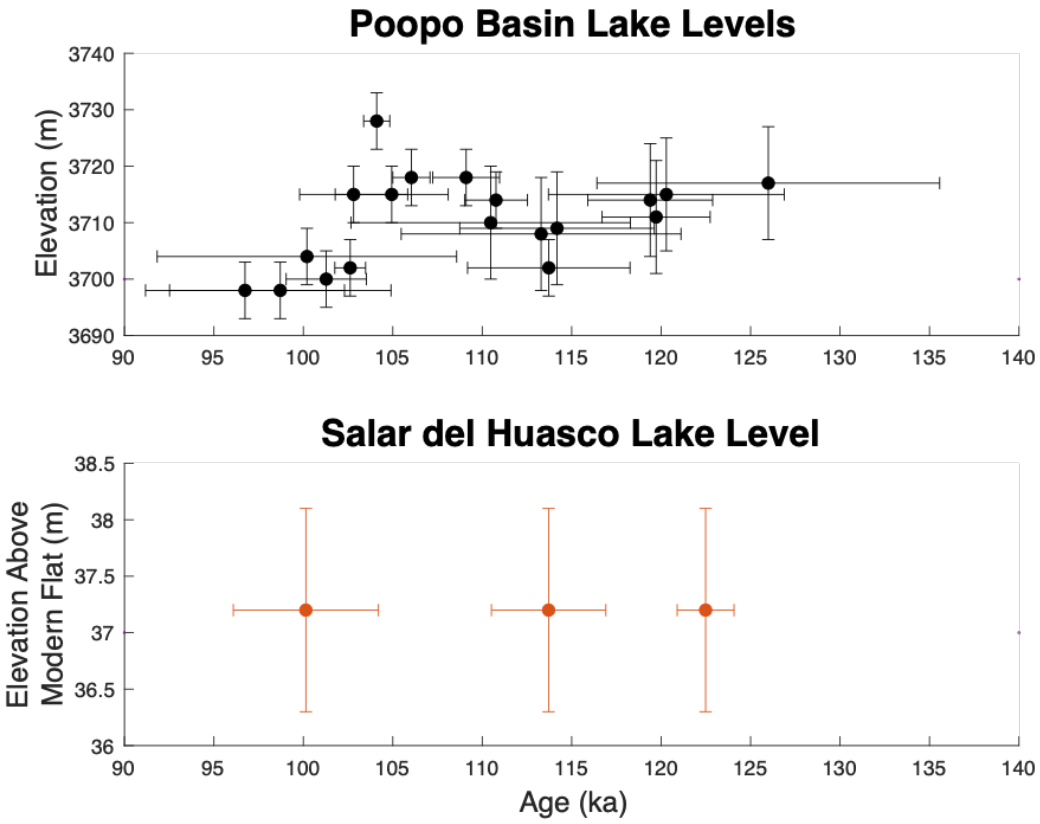

Figure 3-15: Comparison of Placzek et al., 2006 paleo lakeshore reconstructions from the Poopo Basin with the Salar del Huasco data generated between 140-90 ka.

Figure 3-15 shows the few age versus elevation measurements generated for the Salar del Huasco during the last interglacial and into the last glaciation, against the lake level data collected for the Poopo basin by Placzek et al. (2006). Although the three Salar del Huasco dates generated are insufficient to build a lake level chronology for this period, the fact that they align well in time with a suggested (but contentious) lake level highstand in a neighboring basin provides a useful point of consistency between our work and other literature.

Chapter 4

Discussion

4.1 U/Th Data Implications

Samples CYC16-061, CYC16-062 and CYC16-064 (Figures 3-2, 3-3 and 3-4, respectively) were selected as key samples to be studied because of their unique layered structures (discussed in Introduction Section 1.3). Generally, tufa samples are far more homogenous in color and normally represent only a very short depositional timeframe. This means in order to generate lake level records, many tufa samples at different elevations need to be collected and dated.

CYC16-061 spans a greater time range than either of the other key samples studied. Figures 3-5 and 3-6 show that this tufa sample represents ages from 125-105 ka and 19-12 ka. Near the bottom of this sample shown in Figure 3-2 (the layers deposited between 125-105 ka), tufa layers are markedly less evenly deposited than in CYC16-062 or 064, which span dates only from the most recent deglaciation. These uneven depositional layers may be the result of uneven tufa growth at the time, uneven weathering of the tufa layers once they have been deposited, or different morphologies of micro-organisms at each highstand. Uneven tufa growth layers seem less likely here, as the minute laminae within the older tufa are all of uniform thickness with growth layers which mimic the uneven surface of the sample, even though the overall shape is less flat in geometry. Alternatively, older tufa samples are less frequently found as they are often re-dissolved or weathered after deposition, perhaps providing

support for the idea that the uneven depths of these older tufa layers are a result of post-formation partial weathering. In further support of this weathering hypothesis is the fact that CYC16-061 and CYC16-062 occurred at the same elevation, so we might have expected them to be deposited simultaneously. It may be that the basaltic rock on which CYC16-062 formed also once had older tufa deposits, but these weathered preferentially to the CYC16-061 samples that retain some of the older tufa. However, the even thickness of the laminae within these layers, and the lack of evidence for erosion when initially collected, weaken this hypothesis. Finally, this uneven geometry may be due to the microbes involved in forming the tufas during this older lake level highstand favoring mound-like structures (which is supported by the even laminae within the layers), while the more modern microbes may have preferentially formed flat layers.

While CYC16-061 is a particularly interesting tufa sample as it contains these unusual older dates, it also provides a good example of the possible pitfalls of applying U/Th dating to tufas. As illustrated in Figure 3-6, the two dates closest to the top of the sample defy stratigraphic order. This indicates that the top of sample CYC16-061 did not remain a closed U-series decay system after deposition. Diagenesis leads to the leaching of uranium isotopes from the top of this sample, increasing the measured $^{230}Th/^{234}U$ activity ratio in this part of the sample. Therefore, diagenesis of this tufa portion – which, by stratigraphy, we know must be younger than tufa further from the sample top – means apparently older ages are found at the top of the sample rather than further down. As the top dates from the sample were impacted by open U-system behavior and therefore were not included in our age model, the top 8 mm of CYC16-061 is not well constrained in age. In future work, performing XRD analysis on the sample to determine if there is a change in minerology could help to constrain the depth horizon at which diagenesis occurred, as some forms of carbonate such as aragonite are more susceptible to diagenesis than other forms such as calcite.

Although only one depositional hiatus is reported in CYC16-061, Figure 3-6 suggests there may be another depositional hiatus between 16-14 ka. To test if this deposition hiatus is merely a sampling bias or is actually present, CYC16-061B(R)

was drilled between the 16 ka and 14 ka holes. Unfortunately, this powder could not be dated before lab operations were shut down, but future work should determine the age at this depth to understand if a depositional hiatus occurred or not.

Similarly, sample CYC16-062 may also contain a depositional hiatus, or may indicate a sampling bias. Sample CYC16-062 was deposited at approximately the same elevation as CYC16-061, but experienced deposition over 17-13 ka. As shown in Figure 3-7, the vast majority of the sample was deposited between 17-15 ka, with only the top-most tufa layer containing CYC16-062(C) occurring around 13 ka. This two thousand year leap may indicate a rapid decrease in deposition rate, or may be indicative of a hiatus in deposition. As seen in Figure 3-3, there is a visible color change between the tufa layer containing the top hole CYC16-062(C) and the layer containing hole CYC16-062(H), which might indicate a depositional hiatus. However, earlier color changes in this same tufa did not correspond to a hiatus as the rest of the sample seems to have been continuously deposited over two thousand years. In the future, another U/Th date should be taken between CYC16-062(C) and CYC16-062(H) to determine if a hiatus occurred, or if the rate of deposition merely increased.

Interestingly, sample CYC16-064 seems to have been entirely deposited between 15.5-14 ka – the possible depositional hiatus in CYC16-061 and CYC16-062 – and occurs at a 10 m lower elevation than the other two key samples. As shown in Figure 3-8, all layers dated from CYC16-064 had fairly low 2σ age uncertainties besides the deepest replicate date generated from holes CYC16-064(A) & CYC16-064(D). As seen in Figure 3-4, these holes occurred in a tufa layer discrete from the rest of the sample. This layer had exceptionally high detrital ^{232}Th, which implies a high detrital ^{230}Th concentration, increasing the age uncertainties for dates generated with U/Th dating. As explained in the Introduction Section 1.4, ^{232}Th is a (relatively) stable isotope that can serve as a tracer for the amount of detrital thorium incorporated into the tufa when formed. The ^{232}Th content in the tufa layer containing holes CYC16-064(A) & CYC16-064(D) was measured at 79 ng/g, whereas typical values for the rest of the sample ranged from 10-18 ng/g. This high ^{232}Th content suggests large amounts of ^{230}Th were incorporated into this tufa layer on formation, meaning age uncertainties

are high. If we enforce stratigraphic order in our samples, the oldest layer was likely formed at the upper end of the 2σ uncertainty, and must be older than 14.8 ka to stratigraphically agree with hole CYC16-064(E).

Generally, the depth versus age data collected from samples CYC16-061, CYCY16-062 and CYC16-064 obey stratigraphic order and provide a good framework from which to build our COPRA stable isotope versus age models and our lake level elevation history. Sample CYC16-061 exhibits some open uranium system behavior in its top 8 mm, meaning this period of deposition cannot be well constrained in time. The deepest layer of sample CYC16-064 had high detrital thorium content, leading to large MSWD-corrected uncertainties. However, by enforcing stratigraphic order, we conclude that this tufa layer likely formed between 16-15 ka. In the future, more tufa sampling in CYC16-061 and CYC16-062 should be conducted to resolve the presence or absence of depositional hiatuses between 16-13 ka.

4.2 Stable Isotope Data Implications

As seen in Figure 3-9, the ikaite CYC16-067 had reasonably similar δ^{18}O values but a markedly lighter δ^{13}C range than the rest of the tufas studied. As shown in Table 3.1, CYC16-071 had the lowest elevation of all of the tufa samples studied, forming 7m lower than the next lowest tufa sample. This low elevation makes sense as the sample is an ikaite, and these carbonates often form within sediments or at the sediment/water interface. The low elevation of the ikaite and proximity to sediments may mean it was exposed to isotopically light carbon due to organic matter respiration within the sediments (Kodina et al., 2003), resulting in the lighter δ^{13}C values we observe. Besides the ikaite sample, Figure 3-9 illustrates that the remainder of the Salar del Huasco tufas had similar ranges of δ^{18}O and δ^{13}C values. CYC16-061, CYC16-062 and CYC16-064 all had δ^{18}O ranges from -0.5 to 2 permil and δ^{13}C ranges of 4-6 permil VPBD. As shown in Figure 3-10, these samples all spanned almost this complete range of values.

Importantly, trends for δ^{18}O and δ^{13}C values in CYC16-061, CYC16-062 and

CYC16-064 are all consistent with the Salar del Huasco being a historically closed basin lake system. Figure 3-10 shows a positive correlation between δ^{18}O and δ^{13}C values, as well as enriched δ^{18}O and δ^{13}C values, and an almost 3 permil variability between δ^{18}O values in single samples. Enriched δ^{18}O (when compared to local precipitation) and δ^{13}C values are thought to be typical of closed lake basins that experience a high amount of evaporative enrichment (Deocampo, 2010; Aravena et al., 1999). Similarly, closed basin lake systems are expected to have a strong positive correlation between δ^{18}O and δ^{13}C, as to establish this covariance long residence times within a basin are necessary (Talbot, 1990). Finally, the several permil variability in δ^{18}O over the samples is characteristic of a closed basin lake, as closed lake systems experience greater fluctuations in water isotopic balance than open system lakes (Talbot, 1990).

Sample CYC16-064 showed the same δ^{18}O and δ^{13}C range as the other samples, although it represented a much shorter time span, perhaps indicating aliasing of our data. Aliasing occurs when a data trend is undersampled such that its signal becomes indistinguishable from a signal with a longer period. In this case, all samples had the same depth between stable isotope drill holes, but as CYC16-064 was deposited much faster (see Figure 3-8), the distance in time between each of these drill holes was much shorter. As CYC16-064 shows a similar trend to stable isotope measurements from other samples which were more spread out through time, these signals may be aliases of each other. More fine stable isotope sampling may be necessary to resolve if the trends observed here are real or are a result of undersampling.

The stable isotope data versus depth within sample were plotted in Figure 3-11, and again show strong covariance between δ^{18}O and δ^{13}C along the depth of the samples in most cases. CYC16-062 and CYC16-064 both had reasonable covariance between δ^{18}O and δ^{13}C, with δ^{18}O fluctuating more between individual drill holes. The higher fluctuation of δ^{18}O is reasonable, as this input can be quickly altered by precipitation changes while δ^{13}C values are more consistent in a closed lake system. CYC16-061A showed very close correlation between δ^{18}O and δ^{13}C until approximately the top 4 mm of the sample, at which point δ^{18}O increased far more than

δ^{13}C. This cannot be explained by precipitation, which tends to be isotopically light. However, as we know this portion of the sample experienced uranium diagenesis, this may be indicative of stable isotope diagenesis occurring, and the carbonate incorporating oxygen from water which is more evaporatively enriched than the original lake. For this study, we assumed stable isotope diagenesis did not occur, but in future XRD analysis to determine the minerology of the sample would help to support or reject this assumption.

Figure 3-13 shows the uneven deposition rates and changes in stable isotope values throughout time. Having used COPRA to generate a depth vs age model (example seen in Figure 3-12) for samples CYC16-061, CYC16-062 and CYC16-064, a stable isotope data versus age plot (Figure 3-13) was produced. The tight and then sparse grouping of data points along the time axis shows that while depth spacings for stable isotope measurements were the same across every sample, depositional rates varied between and within each sample, meaning we have unevenly sampled with respect to time. As discussed above, the close spacing of data points in Figure 3-13 indicates that CYC16-064 had a very fast rate of deposition. CYC16-062 had a similarly fast rate of deposition at its midpoint, before slowing significantly from 15-13 ka (again, this may be due to a sampling bias mentioned earlier failing to identify a hiatus). The deposition rate of CYC16-061 varied heavily through time, but at all points seems to have been slower than both CYC16-062 and CYC16-064. Trends in stable isotope values through time were not examined closely, as these may be the result of undersampling and aliasing, discussed above.

In Figure 3-13, the oldest and youngest predicted dates for the stable isotope measurements have significantly greater 2σ error bars than the dates that occur in the middle. This is a result of the COPRA age modelling system and is mirrored in Figure 3-12. Dated points that are flanked by other age estimates are more tightly constrained in time, whereas dated points at the top and bottom of samples are less well constrained in time. Though the absolute ages of the stable isotope measurements are sometimes highly uncertain, stratigraphic order means that the dashed line showing trends in our samples must be accurate even if the absolute timings or rates

of these trends are uncertain. The age uncertainty is particularly prevalent in the earliest CYC16-061 ages, as the top 8 mm of this sample are not age constrained.

While we can compare the 20-10 ka depositional events fairly well, δ^{18}O and δ^{13}C in the older paleolake are not captured sufficiently to compare. Only two of the stable isotope holes drilled in CYC16-061 represent older ages, meaning little can be said about trends in stable isotopes between the 127 ka and 98 ka points. However, by comparing the time horizons, we can see that the older paleolake within the Huasco basin was less enriched in δ^{18}O and δ^{13}C than during the more recent paleolake event. This may be indicative of different water chemistry in this older lake, or possibly a different balance between precipitation and evaporation, leading to less δ^{18}O and δ^{13}C evaporative enrichment.

Overall, the stable isotope data provides strong evidence that the Salar del Huasco exists as a closed basin lake system. The strong correlation between, and enrichment of, δ^{18}O and δ^{13}C measurements, combined with the multiple permil variability of δ^{18}O, all point to Salar del Huasco being a hydrologically closed basin. Though the trends in δ^{18}O and δ^{13}C in age for some of our samples are not well constrained, future work that increases the sampling rate for U/Th dating will reduce age uncertainties, allowing for clearer patterns in stable isotope variation and deposition rate.

4.3 Salar del Huasco Paleolake Levels

Having used the stable isotope data to confirm that the Salar del Huasco is a closed system basin even during lake highstands, we can now use the elevations and ages of our key tufa samples to make a preliminary reconstruction of lake levels through time. Shown in the bottom panel of Figure 3-14, our tufa samples suggest a lake level highstand at 37 m from 18-15 ka – and potentially having arisen as early as 19 ka, based on a single U/Th date from CYC16-061B. The lake then appears to have decreased in height by 10 m, during which time CYC16-064 was deposited, before increasing to 37 m above the modern flat from 14-12 ka. As the top 8 mm of CYC16-061 are undateable due to diagenesis, it is possible that this most recent highstand

continued past 12 ka. In addition, sample CYC16-061 provides evidence for lake level highstands between 124-104 ka (see Figure 3-15), although too few samples exist to suggest if this is a continuous highstand or multiple discrete events.

As noted in the U/Th dating discussion section, it is currently unclear how "real" the 10 m lake level decrease from 15-14 ka actually is. Both samples CYC16-061 and CYC16-062 have dates that bracket this period (see Figures 3-6 and 3-7), but it is unclear if these tufas experienced a depositional hiatus over this period, or if these periods just indicate a decrease in deposition rate. In future work, CYC16-061B(R) should be dated, and a U/Th powder should be drilled at the 3-4 mm depth in CYC16-062, to determine whether deposition occurs in these samples from 15-14 ka. Despite this uncertainty in lake elevation from 15-14 ka, our tufa records provide evidence for paleolake levels above modern from at least 18-12 ka. More sampling should be done on these tufas and others from Salar del Huasco, in order to better resolve a full lake level chronology for the last deglaciation.

4.4 Regional Hydrological Comparison

In addition to plotting the Salar del Huasco lake level record generated by this study, Figure 3-14 also shows evidence for increased precipitation across various sites in the Altiplano generated by other studies (Gayo et al., 2012; Placzek et al., 2006; Quade et al., 2008). Each of these studies indicate an increase in local precipitation levels beginning around the last deglaciation and persisting for several thousand years. Gayo et al. find evidence for paleo wetlands in the Atacama desert beginning as early as 17.5 ka, and in earnest for the periods between 16-14 and 12-11 ka. Placzek et al. used tufa radiocarbon and U/Th dating to reconstruct lake level elevations in the Salar de Uyuni and Poopo and Coipasa basins, which neighbor the Salar del Huasco. Placzek et al.'s data shows clear evidence for increased lake levels between 18-11 ka, and the authors suggest a decrease in elevation occurred from 14-13 ka. Finally, dated paleo wetland sediments from the central Atacama suggest water table heights that were 27 m above modern between 16-10 ka, with a possible brief drop at 13 ka (Quade et

al., 2008).

In broad terms, the other palaeohydrological reconstructions shown in Figure 3-14 agree with the basic findings of our Salar del Huasco lake level elevations. These other studies all show an increase in water levels following the LGM, however, Placzek and Gayo suggest an onset around 18 ka and Quade around 17 ka, while our data for Huasco suggests increased lake levels might have occurred as early as 19 ka. However, this 19 ka estimate is based on a single data point with significant associated error – which may have occurred as early as 17.5 ka. Therefore, to a first degree, all of these palaeohydrology reconstructions indicate increased precipitation beginning around the same time. Furthermore, the Placzek and Gayo papers both suggest that this increased precipitation terminated between 12-11 ka, which is in line with our tufa reconstructions.

Interestingly, all of the other papers predict a lake level decrease in the middle of this period – mirroring the possible drop we observe in our preliminary lake level reconstruction. However, while our potential lake level decrease appears between 15-14 ka, each of the other studies predict more recent dates for the intermittent lake level drop, generally from 14-13 ka. This discrepancy can be interpreted in a number of ways. Firstly, it could indicate that Huasco experiences a drop in precipitation at a time when the other areas do not, which could potentially indicate that the Uyuni basin receives its rainfall from a more northern latitude at this time. Alternatively, as noted above, it is currently unclear how "real" the decrease in our lake level elevation is, and more sampling is needed to resolve whether lake level height is truly lower. It may be that upon further investigation, our lake level record does not contain a decrease from 15-14 ka at all. Similarly, the evidence from Quade, Placzek and Gayo for decreases in water level is far from conclusive. Gayo and Quade rely on a lack of leaf litter deposits and sediment deposits respectively as evidence for a decrease in water levels, but this evidence could potentially be explained by erosion or outside factors that do not necessarily indicate drops in water levels. Placzek et al. draw a lake level elevation line that shows a lake level decrease, however, outlying U/Th and radiocarbon dates at far higher elevations occur during this intermission, indicating that

this lake level reconstruction is uncertain. Finally, the respective lag time between climatic drying and a decline in water availability in each environment may differ significantly, which could explain the 1 ka discrepancy between the possible Huasco lake decrease and the projected drop in other areas. In groundwater-dominated systems like the wetlands Gayo and Quade discuss, there could be a substantial lag, while the small, precipitation-reliant Huasco basin may respond more quickly. Therefore, it's possible that these potential decreases actually represent the same climatic event, but that the signals of this possible climatic drying are delayed in wetland environments. Due to the many caveats in both our lake level reconstructions and those of Gayo et al., Placzek et al. and Quade et al., the discrepancies between the water level decrease timings should not be a high cause for concern at this time.

Finally, sample CYC16-061 also provides evidence for a lake highstand between 125-105 ka, which is corroborated by tufa deposits from the Poopo Basin. As shown in Figure 3-15, Placzek et al. present tufa samples from the Poopo Basin that indicate a lake highstand occurred between 125-97 ka (Placzek et al., 2006), and roughly correspond to the period of observed lake level highstands in the Salar del Huasco. Our data therefore supports the hypothesis of Placzek et al. that this 125-97 ka highstand was present as far south as the Uyuni Basin, and suggests that studying the Salar del Huasco further could provide evidence that resolves the current scientific dispute between Baker & Fritz and Placzek et al., mentioned in the Introduction Section 1.2. Although the three U/Th dates generated from CYC16-061 do not contain enough information to create a lake level history with confidence, the fact that they align well with the Placzek data is a promising indication that the Salar del Huasco and neighboring basins experienced synchronous lake level highstands over a long period of time. More generally, it appears clear that the two most recent hydrologic maxima in the Altiplano occurred during the last deglaciation and in the period from 120-100 ka. While the deglacial highstand likely relates to Northern Hemisphere cooling (Heinrich events) and a southward shift of SASM rains, the causes behind the 120-100 ka highstand(s) remain unclear.

Chapter 5

Conclusion

Our in-depth studies of three layered tufa deposits from the Salar del Huasco basin yielded some key conclusions about the basin's lake level history and hydrology through time. Firstly, our stable isotope data indicate that the Salar del Huasco is a historically closed basin system. As the basin is relatively small, this means it reflects lake level variations and water chemistry changes that are influenced only by local hydrological changes. This may allow for an understanding of precipitation changes through time more tightly constrained by latitude than that provided by the neighboring Titicaca-Uyuni basin. The unusual layered depositional pattern of the tufas collected from this site contain multiple depositional events, allowing a high number of lake level elevation over time points to be generated from a single tufa sample. Lake level highstands occurred between 125-105 ka and from 19-12 ka, and are broadly consistent with palaeohydrological data from a variety of sites in the region. The Salar de Uyuni & Poopo Basin lake level reconstructions by Placzek et al. correlate particularly well with the Huasco highstand data presented here, reinforcing the idea that the Salar del Huasco data can be compared to the larger Titicaca-Uyuni basin data to resolve whether signals from the Uyuni basin are due to increased precipitation at this latitude, or were being driven by precipitation in more northern areas of the extensive Titicaca-Uyuni basin. Preliminarily, our data supports Placzek et al.'s hypothesis that increased rainfall occurred as far south as 20.2°S from 120-100 ka, and therefore, Salar del Huasco lake level reconstructions have the potential to

resolve an active debate in scientific literature.

In the future, continued work on the collected tufa samples will better constrain the lake level elevation chronology, reduce age modelling uncertainties, and increase confidence in the accuracy of our U/Th dates. By dating a greater number of tufa samples collected at different elevations, and by addressing the current gaps in our sampling of CYC16-061 and CYC16-062 to resolve the presence of a hiatus or a change in deposition rate, we will generate a more accurate model for lake level reconstructions. By increasing the frequency of U/Th sampling in our tufa samples, interpolated age models generated through COPRA will have lower associated uncertainties, and will allow us to better understand depositional rates and δ^{18}O and δ^{13}C patterns through time. Finally, XRD should be used to determine the mineralogy of our tufa samples, and trace element analysis applied to determine the water chemistry producing these deposits. Through this, we will not only understand the susceptibility of different portions of tufa to diagenesis, but also begin to resolve how lake chemistry changed throughout time. By answering these questions, we will further improve our understanding of the palaeohydrology of the Salar del Huasco, and its reflection of regional precipitation patterns over at least the past one hundred and thirty thousand years.

Bibliography

Aravena, R., Suzuki, O., Peña, H., Pollastri, A., Fuenzalida, H., & Grilli, A. (1999). Isotopic composition and origin of the precipitation in Northern Chile. *Applied Geochemistry, 14*(4), 411–422. https://doi.org/10.1016/S0883-2927(98)00067-5

Baker, P. A., & Fritz, S. C. (2015). Nature and causes of Quaternary climate variation of tropical South America. *Quaternary Science Reviews, 124*, 31–47. https://doi.org/10.1016/j.quascirev.2015.06.011

Bender, M. L. (2013). *Paleoclimate*. Princeton: Princeton University Press.

Breitenbach, S. F. M., Rehfeld, K., Goswami, B., Baldini, J. U. L., Ridley, H. E., Kennett, D. J., ... Marwan, N. (2012). COnstructing Proxy Records from Age models (COPRA). *Climate of the Past, 8*(5), 1765–1779. https://doi.org/10.5194/cp-8-1765-2012

Chen, C. Y., McGee, D., Woods, A., Pérez, L., Hatfield, R. G., Edwards, R. L., ... Rodbell, D. T. (2019). U-Th dating of lake sediments: Lessons from the 700 kyr sediment record of Lake Junín, Peru. https://doi.org/10.31223/osf.io/c765k

Cruz, F. W., Karmann, I., Viana, O., Burns, S. J., Ferrari, J. A., Vuille, M., ... Moreira, M. Z. (2005). Stable isotope study of cave percolation waters in subtropical Brazil: Implications for paleoclimate inferences from speleothems. *Chemical Geology, 220*(3), 245–262. https://doi.org/10.1016/j.chemgeo.2005.04.001

Deocampo, D. M. (2010). The Geochemistry of Continental Carbonates. In A. M. Alonso-Zarza & L. H. Tanner (Eds.), *Developments in Sedimentology* (Vol. 62, pp. 1–59). Amsterdam: Elsevier. https://doi.org/10.1016/S0070-4571(09)06201-3

Fornari, M., Risacher, F., & Féraud, G. (2001). Dating of paleolakes in the central Altiplano of Bolivia. *Palaeogeography, Palaeoclimatology, Palaeoecology, 172*(3), 269–282. https://doi.org/10.1016/S0031-0182(01)00301-7

Fritz, S. C., Baker, P. A., Lowenstein, T. K., Seltzer, G. O., Rigsby, C. A., Dwyer, G. S., ... Luo, S. (2004). Hydrologic variation during the last 170,000 years in

the southern hemisphere tropics of South America. *Quaternary Research, 61*(1), 95–104. https://doi.org/10.1016/j.yqres.2003.08.007

Garcia, M., Raes, D., Jacobsen, S.-E., & Michel, T. (2007). Agroclimatic constraints for rainfed agriculture in the Bolivian Altiplano. *Journal of Arid Environments, 71*(1), 109–121. https://doi.org/10.1016/j.jaridenv.2007.02.005

Garreaud, R., Vuille, M., & Clement, A. C. (2003). The climate of the Altiplano: Observed current conditions and mechanisms of past changes. *Palaeogeography, Palaeoclimatology, Palaeoecology, 194*(1), 5–22. https://doi.org/10.1016/S0031-0182(03)00269-4

Gayo, E. M., Latorre, C., Jordan, T. E., Nester, P. L., Estay, S. A., Ojeda, K. F., & Santoro, C. M. (2012). Late Quaternary hydrological and ecological changes in the hyperarid core of the northern Atacama Desert (∼21°S). *Earth-Science Reviews, 113*(3), 120–140. https://doi.org/10.1016/j.earscirev.2012.04.003

Geyh, M. A., Grosjean, M., Núñez, L., & Schotterer, U. (1999). Radiocarbon Reservoir Effect and the Timing of the Late-Glacial/Early Holocene Humid Phase in the Atacama Desert (Northern Chile). *Quaternary Research, 52*(2), 143–153. https://doi.org/10.1006/qres.1999.2060

Hernández, K. L., Yannicelli, B., Olsen, L. M., Dorador, C., Menschel, E. J., Molina, V., ... Jeffrey, W. H. (2016). Microbial Activity Response to Solar Radiation across Contrasting Environmental Conditions in Salar de Huasco, Northern Chilean Altiplano. *Frontiers in Microbiology, 7*, 1857. https://doi.org/10.3389/fmicb.2016.01857

Johnson, E., Yáñez, J., Ortiz, C., & Muñoz, J. (2010). Evaporation from shallow groundwater in closed basins in the Chilean Altiplano. *Hydrological Sciences Journal, 55*(4), 624–635. https://doi.org/10.1080/02626661003780458

Kanner, L. C., Burns, S. J., Cheng, H., & Edwards, R. L. (2012). High-Latitude Forcing of the South American Summer Monsoon During the Last Glacial. *Science, 335*(6068), 570–573. https://doi.org/10.1126/science.1213397

Kodina, L. A., Tokarev, V. G., Vlasova, L. N., & Korobeinik, G. S. (2003). Contribution of biogenic methane to ikaite formation in the Kara Sea: Evidence from the stable carbon isotope geochemistry. In: Stein, R., Fahl, K., Fütterer, D. K., Galimov, E.M., Stepanets, O. V. (Eds.), *Proceedings in Marine Science: Siberian river run-off in the Kara Sea* (pp. 349-374). Amsterdam: Elsevier. https://doi.org/info:doi/10.1016/S1568-2692(03)80045-1

Ludwig, K. R. (2003). Mathematical-Statistical Treatment of Data and Errors for 230Th/U Geochronology. *Reviews in Mineralogy and Geochemistry, 52*(1), 631–656. https://doi.org/10.2113/0520631

Minvielle, M., & Garreaud, R. D. (2011). Projecting Rainfall Changes over the South American Altiplano. *Journal of Climate, 24*(17), 4577–4583. https://doi.org/10.1175/JCLI-D-11-00051.1

Mohtadi, M., Prange, M., & Steinke, S. (2016). Palaeoclimatic insights into forcing and response of monsoon rainfall. *Nature, 533*(7602), 191–199. https://doi.org/10.1038/nature17450

Nunnery, J. A., Fritz, S. C., Baker, P. A., & Salenbien, W. (2019). Lake-level variability in Salar de Coipasa, Bolivia during the past ∼40,000 yr. *Quaternary Research, 91*(2), 881–891. https://doi.org/10.1017/qua.2018.108

Pausata, F. S. R., Li, C., Wettstein, J., Kageyama, M., & Nisancioglu, K. H. (2011). The key role of topography in altering North Atlantic atmospheric circulation during the last glacial period. *Climate of the Past, 7*, 1089–1101. https://doi.org/10.5194/cp-7-1089-2011

Pedley, M., Rogerson, M., & Middleton, R. (2009). Freshwater calcite precipitates from in vitro mesocosm flume experiments: A case for biomediation of tufas. *Sedimentology, 56*(2), 511–527. https://doi.org/10.1111/j.1365-3091.2008.00983.x

Placzek, C. J., Quade, J., & Patchett, P. J. (2013). A 130ka reconstruction of rainfall on the Bolivian Altiplano. *Earth and Planetary Science Letters, 363*, 97–108. https://doi.org/10.1016/j.epsl.2012.12.017

Placzek, C., Quade, J., & Patchett, P. J. (2006). Geochronology and stratigraphy of late Pleistocene lake cycles on the southern Bolivian Altiplano: Implications for causes of tropical climate change. *GSA Bulletin, 118*(5–6), 515–532. https://doi.org/10.1130/B25770.1

Quade, J., Rech, J. A., Betancourt, J. L., Latorre, C., Quade, B., Rylander, K. A., & Fisher, T. (2008). Paleowetlands and regional climate change in the central Atacama Desert, northern chile. *Quaternary Research, 69*(3), 343–360. https://doi.org/10.1016/j.yqres.2008.01.003

Sánchez-Saldías, A., & Fariña, R. A. (2014). Palaeogeographic reconstruction of Minchin palaeolake system, South America: The influence of astronomical forcing. *Geoscience Frontiers, 5*(2), 249–259. https://doi.org/10.1016/j.gsf.2013.06.004

Schwarcz, H. P. (1989). Uranium series dating of Quaternary deposits. *Quaternary International, 1*, 7–17. https://doi.org/10.1016/1040-6182(89)90005-0

Sietz, D., Mamani Choque, S. E., & Lüdeke, M. K. B. (2012). Typical patterns of smallholder vulnerability to weather extremes with regard to food security in the Peruvian Altiplano. *Regional Environmental Change, 12*(3), 489–505. https://doi.org/10.1007/s10113-011-0246-5

Talbot, M. R. (1990). A review of the palaeohydrological interpretation of carbon and oxygen isotopic ratios in primary lacustrine carbonates. *Chemical Geology: Isotope Geoscience Section, 80*(4), 261–279. https://doi.org/10.1016/0168-9622(90)90009-2

Thibeault, J. M., Seth, A., & Garcia, M. (2010). Changing climate in the Bolivian Altiplano: CMIP3 projections for temperature and precipitation extremes. *Journal of Geophysical Research: Atmospheres, 115*(D8), D08103. https://doi.org/10.1029/2009JD012718

Wendt, I., & Carl, C. (1991). The statistical distribution of the mean squared weighted deviation. *Chemical Geology: Isotope Geoscience Section, 86*(4), 275–285. https://doi.org/10.1016/0168-9622(91)90010-T